Electronic Supplementary Material (ESI) for Reaction Chemistry & Engineering.

Supporting Information for:

Thermolysis of 1,3-dioxin-4-ones: Fast generation of kinetic data using in-line analysis under flow

Thomas Durand,[a] Cyril Henry,[a] David Bolien,[a] David C. Harrowven,[a] Sally Bloodworth,[a] Xavier Franck[b] and Richard J. Whitby*[a]

[a] Chemistry, Faculty of Natural and Environmental Sciences, University of Southampton, Southampton, SO17 1BJ, UK. [b] Normandie Université, COBRA, UMR 6014 & FR 3038; Université de Rouen; INSA Rouen; CNRS, 1 rue Tesnière, 76821 Mont-Saint-Aignan Cedex, France.

*Correspondence author: rjw1@soton.ac.uk

CONTENTS

1. Flow Techniques

1.1 Experimental Set-Up and Instrumentation

All flow experiments were carried out on a Vapourtec R2+/R4 series instrument equipped with a stainless steel reactor of 10 mL capacity and 1 mm internal diameter. Reactor heating was achieved by immersion in a Grant Optima™ TXF200 heated bath with high temperature silicone oil. An alpha transmission FT-IR from Bruker was integrated into the flow system thanks to a Harrick DLC2™ demountable liquid flow cell with sodium chloride windows. IR spectra were collected with an interval of 3.75 sec. In-line UV measurements were recorded on an Ocean Optics DH-2000-BAL spectrometer integrated into the flow with a type 583-F Starna® fluorimeter flow cell (1 mm path length, 0.011 mL volume). UV spectra were recorded with an interval of 1.2 sec. Where necessary for off-line reaction analysis, the instrument was connected to a Gilson Prep FC fraction collector (Figure S1.1).

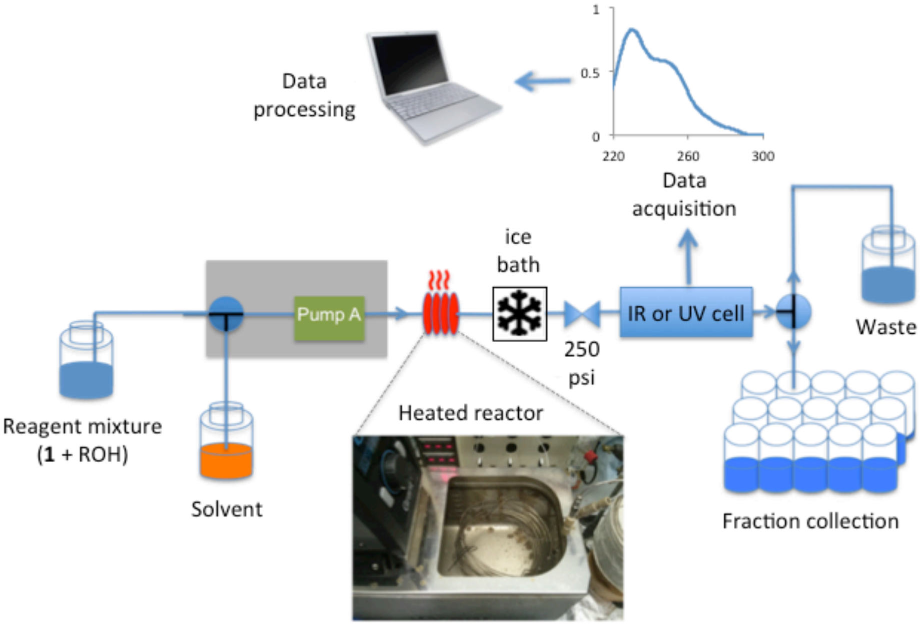

Figure S1.1 Cartoon of flow set-up utilising a single channel (Pump A) of the Vapourtec R series platform and bottle-feed configuration, 10 mL stainless steel reactor submerged in a precision oil bath, ice bath cooling of the reactor efflux, 250 psi back-pressure regulation and in-line IR or UV data acquisition.

1.2 Heat Transfer Experiments

Initial push-out and steady-state kinetic studies upon thermolysis of 2,2,6-trimethyl-4*H*-1,3-dioxin-4-one (**1a**) were performed using the commercial air-heated Vapourtec reactor, according to the general methods of sections 1.3 and 1.4, respectively. Sample data are given in Table S1.1 and Figure S1.2(a) to demonstrate that inefficient heat transfer occurs in air and unequal temperature of the inner and outer reactor coils also results from heat transfer in air; leading to different measured rate constants *k* from the steep and shallow slopes. In comparison, homogeneity of temperature across the reactor results from heat transfer in oil [Fig. S1.2(b)]; resulting in a linear plot of ln[**1a**] *vs.* reaction time. Consistent first-order rate constants were measured across multiple push-out and steady-state experiments, with oil-heating. The precision oil bath-heated stainless steel reactor was employed in all further experiments reported in this document and the main paper.

Kinetic method[a]	air-heated Vapourtec reactor coil	oil-heated stainless steel reactor coil
	$k \times 10^{-3}$ (s^{-1})	$k \times 10^{-3}$ (s^{-1})
Steady-state	3.99	4.92
Push-out	5.86	4.70

Table S1.1 Measured rate constants for thermolysis of 2,2,6-trimethyl-4*H*-1,3-dioxin-4-one (**1a**) in the presence of EtOH (4 equiv.), in acetonitrile at 130 °C. [a] According to the general methods described in sections 1.3 and 1.4. A stepped flow-rate from F_1 = 1 ml min^{-1} to F_2 = 10 mL min^{-1} was used for push-out experiments. In-line UV monitoring was used and data processing carried out by OPA MCR-ALS profiling according to the general method of section 2.1.

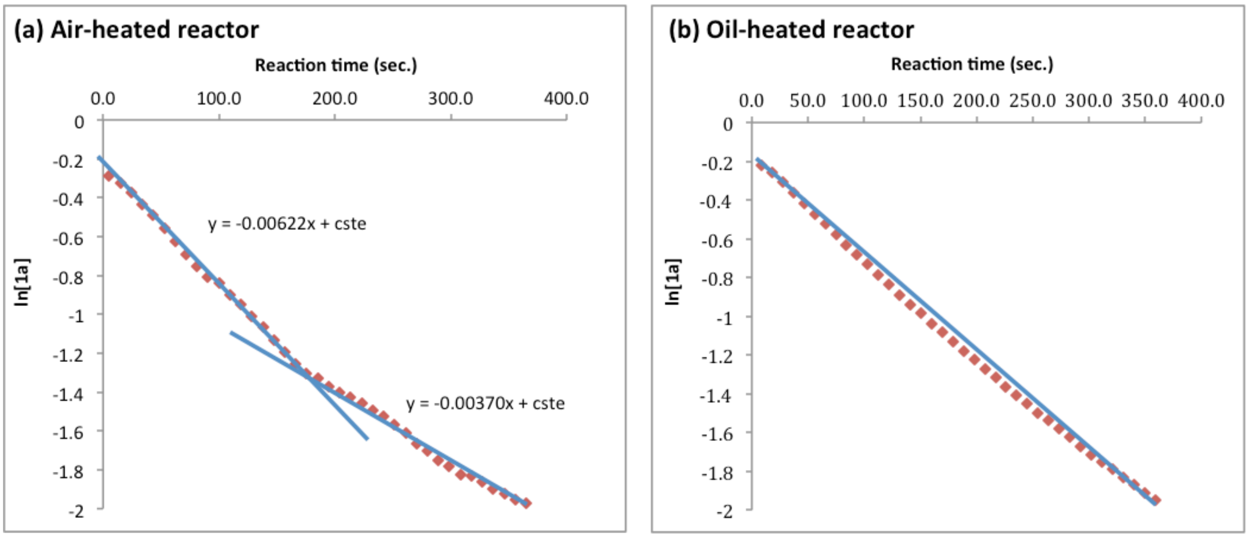

Figure S1.2 Plots of ln[**1a**] *vs*. reaction time (sec.) from push-out kinetic study of the thermolysis of **1a** in the presence of EtOH (4 equiv.) in acetonitrile at 130 °C using (a) Vapourtec commercial air-heated reactor and (b) home-made precision oil bath-heated stainless steel reactor. See section 1.3 for the general experimental method. In-line UV monitoring was used and data processing carried out by OPA MCR-ALS profiling according to the general method of section 2.1.

1.3 General Method of Push-Out Kinetic Studies

A solution of 1,3-dioxin-4-one **1** ([**1**] = 1 mM for UV analysis or 0.015 - 0.3 M for IR analysis) and alcohol (ROH, 4 equiv.) in dry acetonitrile was prepared. Solvent (dry acetonitrile) was then pumped at flow rate F_1 and the reactor set to the requisite temperature. Once the temperature was stable, the feeding valve was switched to the reagent solution, and the mixture exiting the reactor was monitored in-situ until a steady state of conversion was reached. The flow rate was now switched to flow rate F_2 and the reactor efflux was again monitored until a second steady state was reached, upon which the feeding valve was returned to solvent feed. When in-line monitoring revealed no further absorption the flow rate was returned to F_1 and the procedure repeated at the next reaction temperature. Spectroscopic sampling rate was determined by experimental acquisition time/number of spectra recorded and IR and UV data were processed using BORIS chemometric software by calibration-less methods (i) OPA MCR-ALS analysis or (ii) integration of non-overlapping peaks in the UV or IR spectrum with respect to spectroscopic data for 0% and 100% conversion recorded in experiments conducted at 30 °C and 160 °C respectively. Detailed procedures for processing using BORIS are given alongside representative data in section 2.

1.4 General Method of Steady-State Kinetic Studies

A solution of 1,3-dioxin-4-one **1** ([**1**] = 1 mM for UV analysis or 0.015 - 0.3 M for IR and ^{1}H NMR analysis) and alcohol (ROH, 4 equiv.) in dry acetonitrile was prepared. The reactor was set to the requisite flow rate and temperature, and solvent (dry acetonitrile) was then pumped until the temperature was stable. The feeding valve was switched to the reagent solution, and the mixture exiting the reactor was monitored in-situ until a steady state of conversion was reached, upon which spectroscopic data or sample collection was carried out. The feeding valve was then returned to solvent feed and the procedure repeated at the next flow rate, whilst maintaining the same reaction temperature. The completed cycle of multiple experiments (typically five within a cycle, across a range of flow rates in the range 1 mL min^{-1} to 10 mL min^{-1}) was itself repeated several times, each at a different temperature. Each flow rate corresponds to a reaction time calculated from the reactor residence time upon correction for thermal expansion of acetonitrile according to $\text{Flow}_{\text{effective}} = \text{Flow}_{\text{pump set}}(1 + \alpha\Delta T)$ where α = the expansion coefficient of the solvent.[1] IR and UV data were processed using BORIS chemometric software by calibration-less methods (i) OPA MCR-ALS analysis or (ii) integration of non-overlapping peaks in the UV or IR spectrum with respect to spectroscopic data for 0% and 100% conversion recorded in experiments conducted at 30 °C and 160 °C respectively. A typical reagent concentration profile for the steady-state kinetic method is shown in Figure S1.3. Detailed procedures for data processing using BORIS are given in section 2. Analysis of ^{1}H NMR data was carried out manually (see section 4)

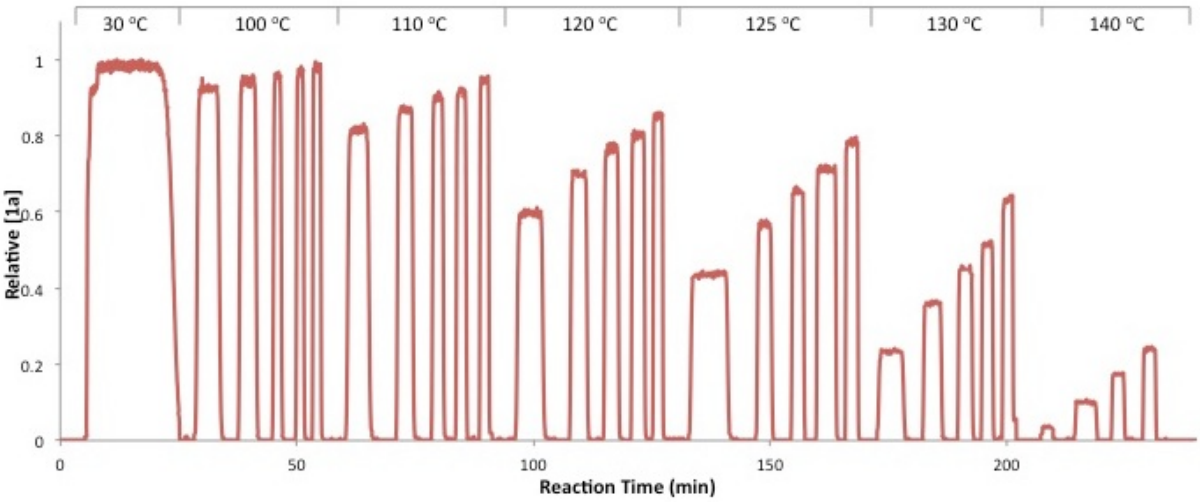

Set Flow (mL min^{-1})	Effective Flow (mL min^{-1})					
	100 °C	110 °C	120 °C	125 °C	130 °C	140 °C
2	2.19728	2.22468	2.25208	2.26578	2.27948	2.30688
3	3.29592	3.33702	3.37812	3.39867	3.41922	3.46032
4	4.39456	4.44936	4.50416	4.53156	4.55896	4.61376
5	5.4932	5.5617	5.6302	5.66445	5.6987	5.7672
7	7.69048	7.78638	7.88228	7.93023	7.97818	-

Figure S1.3 Concentration profile of 2,2,6-trimethyl-4*H*-1,3-dioxin-4-one (**1a**) derived from OPA resolution of IR spectra obtained in-situ from flow thermolysis in the presence of EtOH (4 equiv.) under steady-state conditions. Flow rates within each set of experiments at a given temperature are tabulated.

2. Data Processing

2.1 Orthogonal Projection Approach

OPA multivariate curve resolution of UV and IR spectra was conducted using Bristol Online Reaction Investigation Software (BORIS). The number of spectral components was entered manually and the resolved components optimised through alternating least squares cycles in order to achieve estimated spectra (scaled to unit length) with reliable corresponding concentration profiles of components. Output spectra and concentration profiles were reported in Microsoft Excel, allowing extraction of the reaction time t_r and component concentration data from each constituent spectrum within the overall dataset contributing to the profile. Examples of resolved component spectra and concentration profiles, including overlay of the evolving multi-component spectrum collected in-line, is given for thermolysis of 1,3-dioxin-4-one **1c** (Scheme S2.1) in Figures S2.1-2.2 (UV) and Figure S2.4 (IR).

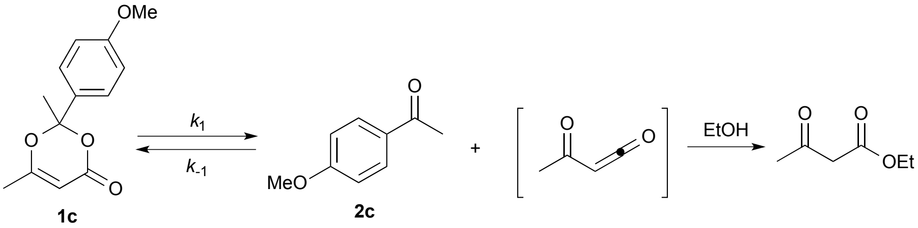

Scheme S2.1 Thermolysis of **1c** and acylketene trapping by EtOH.

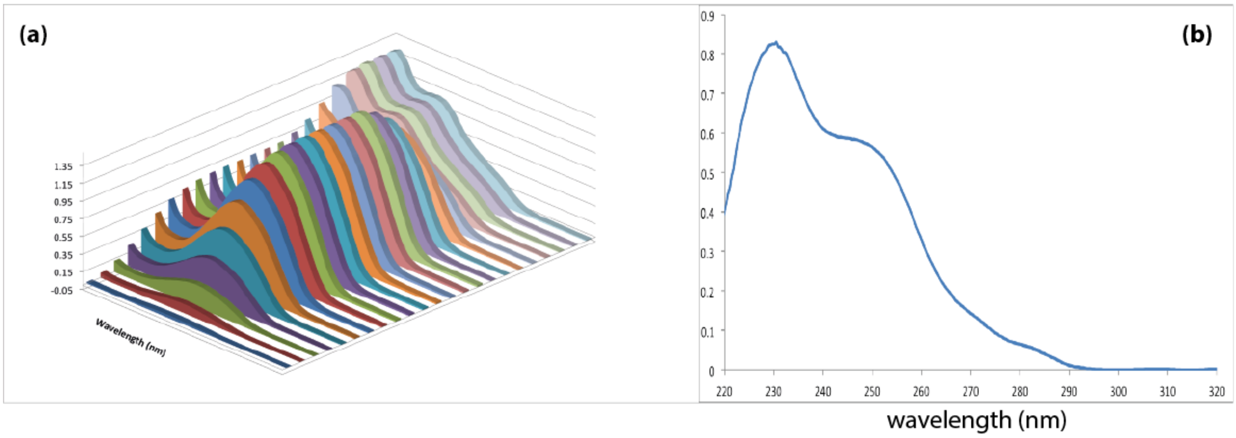

Figure S2.1 (a) UV Dataset including selected spectra collected in-line and (b) representative mixed component UV spectrum. Corresponding resolved component spectra are shown in Figure S2.2 below. Data was collected from push-out flow thermolysis of **1c** in the presence of EtOH (4 equiv.) in acetonitrile and corresponds to the experiment conducted at 85 °C in Table 2, entry 5 of the main paper.

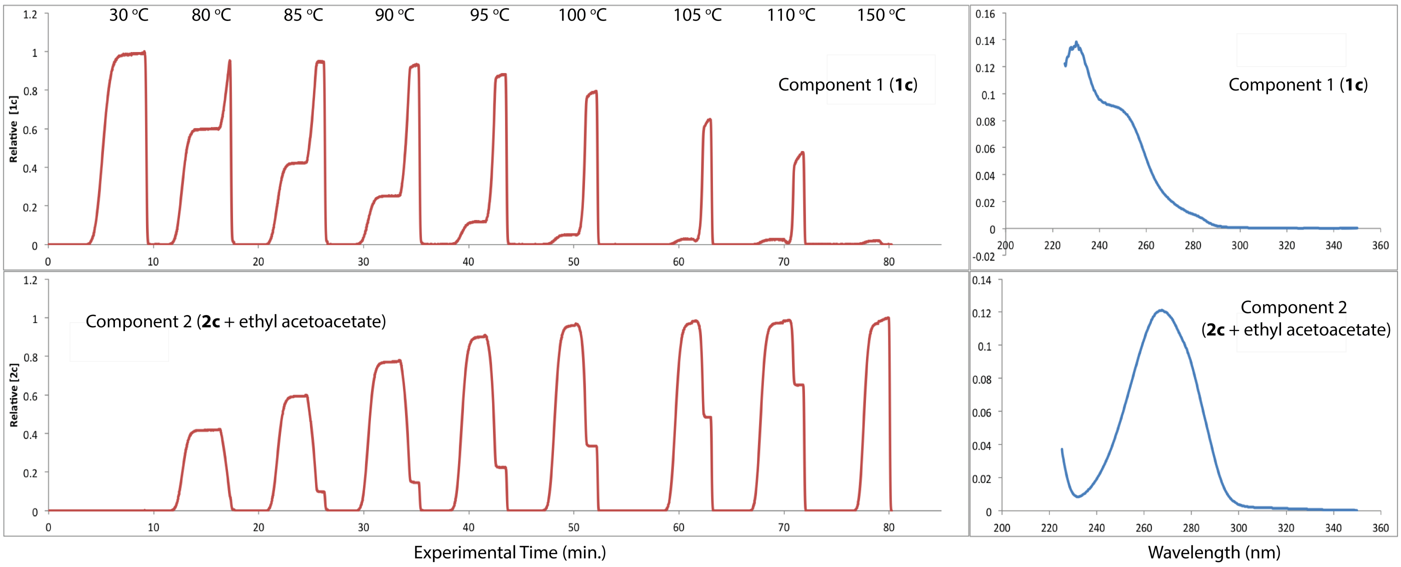

Figure S2.2 OPA (MCR-ALS) resolved concentration profiles and corresponding UV spectra of two components, **1c** and (**2c** + ethyl acetoacetate), determined from push-out flow thermolysis of **1c** in the presence of EtOH (4 equiv.) in acetonitrile. Data corresponds to Table 2, entry 5 of the main paper. **1c** λ_{max} = 234 nm.

p-Methoxyacetophenone (**2c**) and ethyl acetoacetate are identified as a single component in the analysis (Figure S2.2) since their ratio does not change. Attempted three component analysis does not resolve the weakly absorbing ethyl acetoacetate (Figure S2.3).

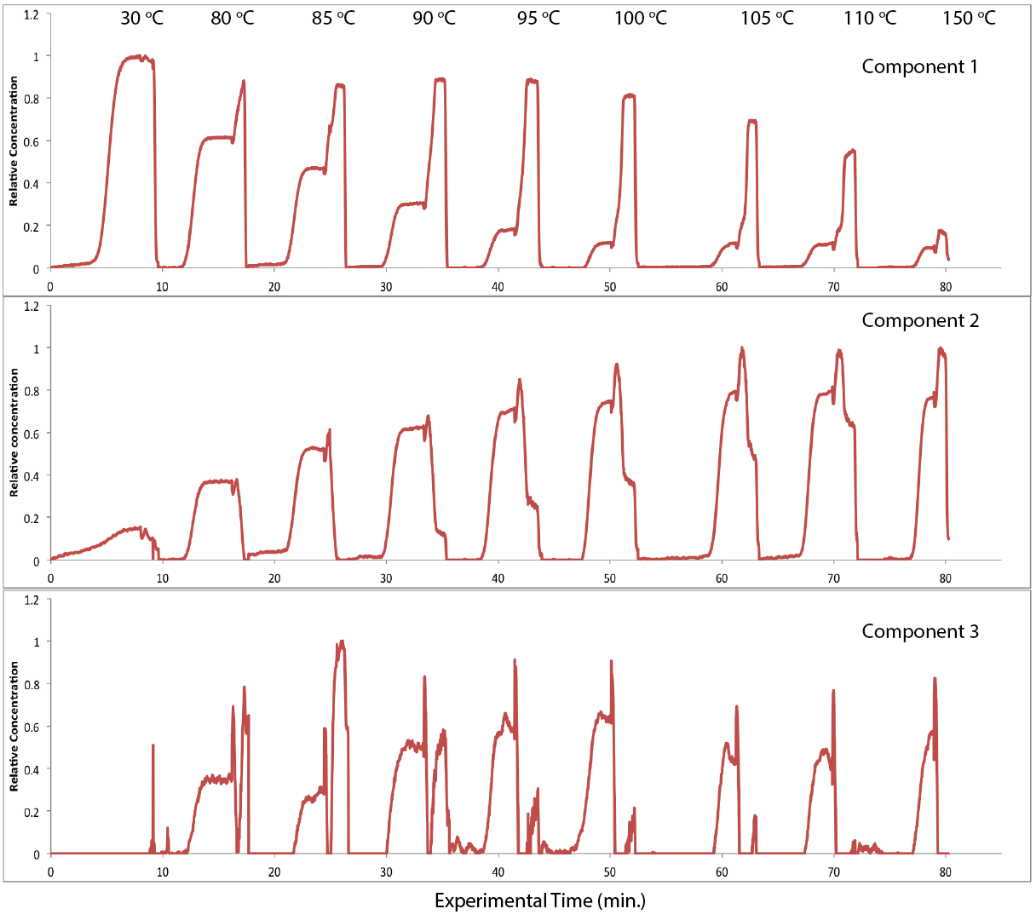

Figure S2.3 Attempted OPA (MCR-ALS) three component resolution of mixed component UV spectra from push-out flow thermolysis of **1c** in the presence of EtOH (4 equiv.), using the same dataset as used for two component resolution shown in Figure S2.2.

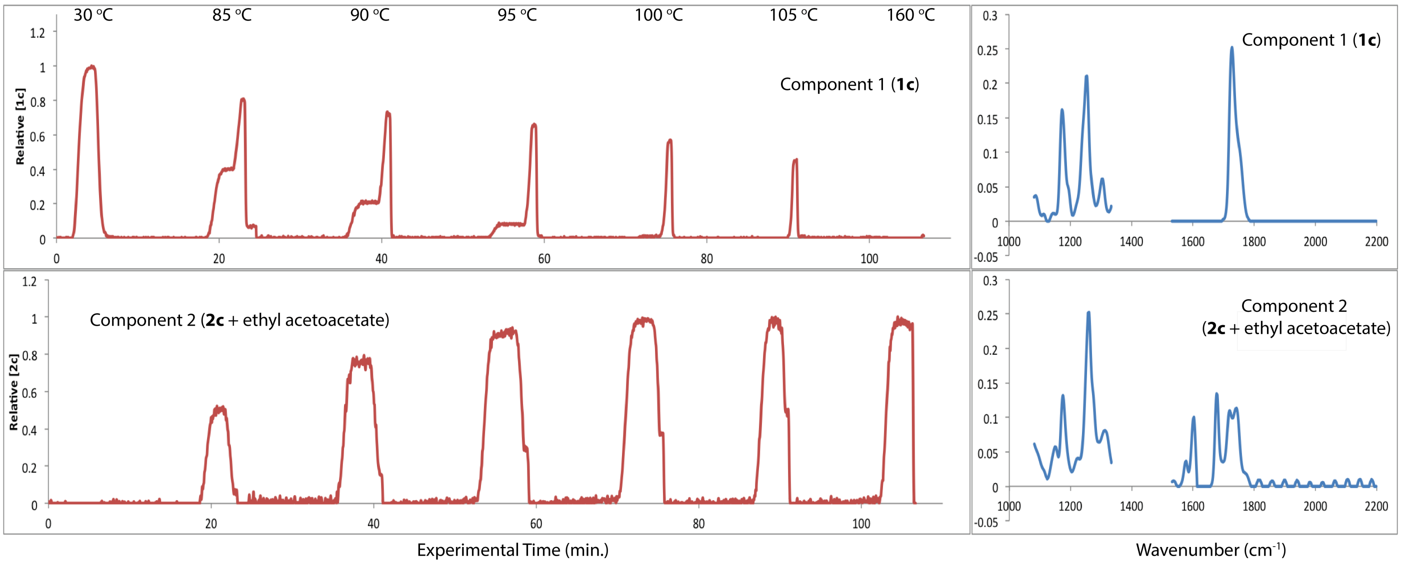

Figure S2.4 OPA (MCR-ALS) resolved concentration profiles and corresponding IR spectra of components **1c** and **2c** determined from push-out flow thermolysis of **1c** in the presence of EtOH (4 equiv.) in acetonitrile. The range of wavelength included in the analysis was selected manually during processing. Data corresponds to Table 2, entry 6 of the main paper.

2.2 Peak Absorbance Profiling

Calculation of [**1**]/[**1**]$_0$ by measurement of UV or IR peak heights above zero was conducted using Bristol Online Reaction Investigation Software (BORIS).

3. Arrhenius Plots

3.1 Table 1 Data

Entry 1: Thermolysis of **1a** in the presence of 4 equiv. EtOH using push-out method, in-line UV analysis and OPA processing. $F_1 = 1$ mL min^{-1} and $F_2 = 10$ mL min^{-1}

Temp. °C	*k*	ln(*k*)	1/T (K^{-1})
100	**0.0002253**	-8.398078488	0.002679887
110	**0.000660526**	-7.322474078	0.002609944
120	**0.001808672**	-6.315162583	0.002543558
130	**0.004704682**	-5.359197028	0.002480466
135	**0.007174536**	-4.937217176	0.00245008
140	**0.010443578**	-4.561768009	0.002420428

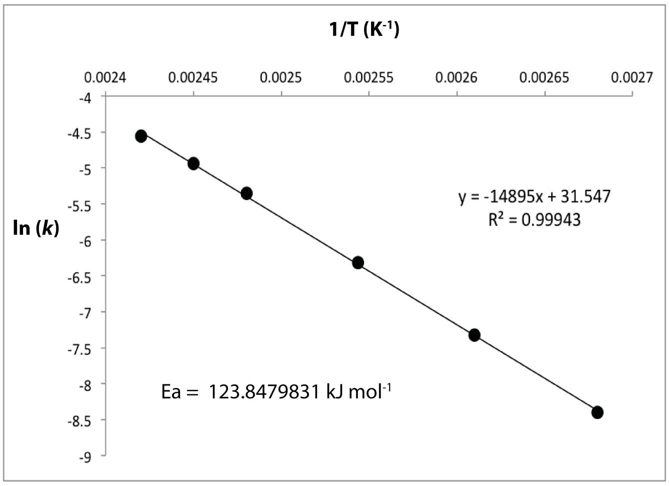

Entry 2: Thermolysis of **1a** in the presence of 4 equiv. EtOH using push-out method, in-line UV analysis and peak absorbance calculation. $F_1 = 1$ mL min $^{-1}$ and $F_2 = 10$ mL min^{-1}

Temp. °C	*k*	ln(*k*)	1/T (K^{-1})
100	**0.000232959**	-8.364649119	0.002679887
110	**0.000646222**	-7.344367152	0.002609944
120	**0.001823268**	-6.307124585	0.002543558
130	**0.004736555**	-5.352445185	0.002480466
135	**0.007071116**	-4.951736968	0.00245008
140	**0.010811649**	-4.527131138	0.002420428

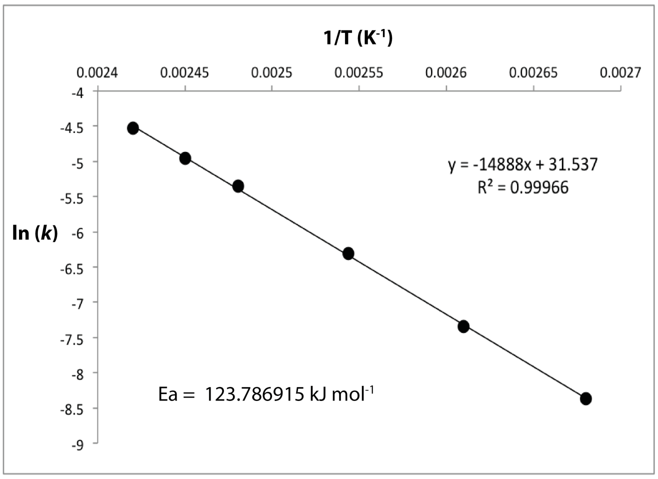

Entry 3: Thermolysis of **1a** in the presence of 4 equiv. EtOH using steady-state method, in-line UV analysis and OPA processing.

Temp. °C	*k*	ln(*k*)	1/T (K^{-1})
100	**0.000237024**	-8.34735054	0.002679887
110	**0.000677258**	-7.297458882	0.002609944
120	**0.001893935**	-6.269098593	0.002543558
130	**0.004921215**	-5.314199899	0.002480466

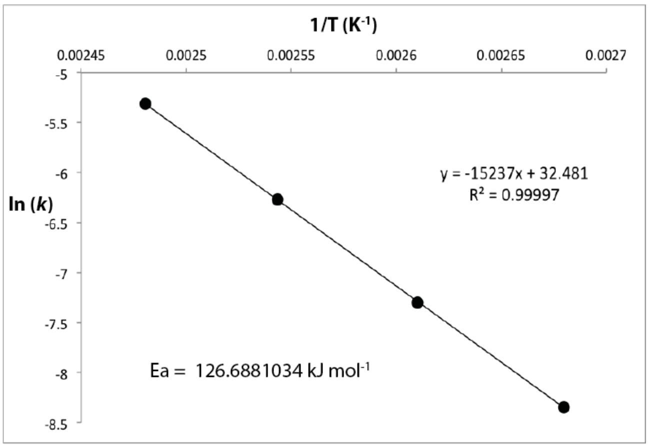

Entry 4: Thermolysis of **1a** in the presence of 4 equiv. EtOH using push-out method, in-line IR analysis and OPA processing. $F_1 = 1$ mL min $^{-1}$ and $F_2 = 10$ mL min^{-1}

Temp. °C	*k*	ln(*k*)	1/T (K^{-1})
100	**0.000268034**	-8.224396356	0.002679887
105	**0.000411167**	-7.796512153	0.002644453
110	**0.000705572**	-7.25650162	0.002609944
115	**0.001167875**	-6.752569378	0.002576324
120	**0.00191556**	-6.257745212	0.002543558
125	**0.003164512**	-5.755756421	0.002511616
130	**0.005064222**	-5.285554785	0.002480466
135	**0.007967575**	-4.832375071	0.00245008
140	**0.011582578**	-4.458253239	0.002420428

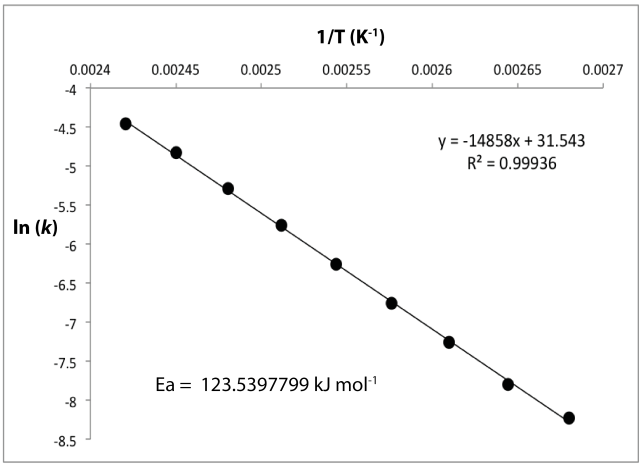

Entry 5: Thermolysis of **1a** in the presence of 4 equiv. EtOH using push-out method, in-line IR analysis and peak absorbance calculation. $F_1 = 1$ mL min $^{-1}$ and $F_2 = 10$ mL min^{-1}

Temp. °C	*k*	ln(*k*)	1/T (K^{-1})
100	**0.000247606**	-8.303671098	0.002679887
105	**0.000382279**	-7.869359666	0.002644453
110	**0.000660319**	-7.322788058	0.002609944
115	**0.001089549**	-6.821991081	0.002576324
120	**0.001804247**	-6.317612091	0.002543558
125	**0.003039696**	-5.795997817	0.002511616
130	**0.004777281**	-5.343883769	0.002480466
135	**0.007564617**	-4.884273495	0.00245008
140	**0.011361675**	-4.4775094	0.002420428

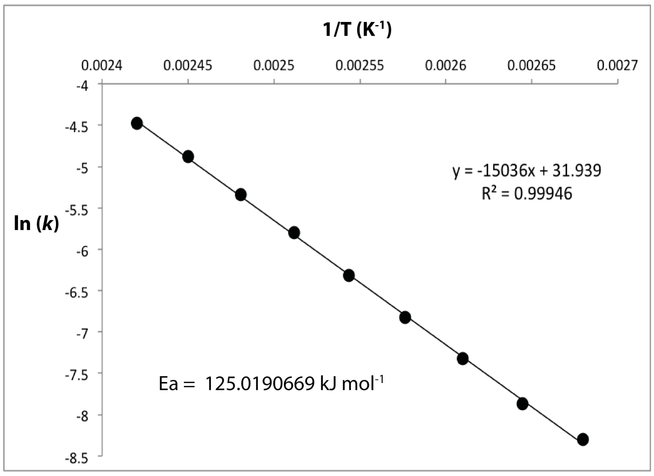

Entry 6: Thermolysis of **1a** in the presence of 4 equiv. EtOH using steady-state method, in-line IR analysis and OPA processing.

Temp. °C	*k*	ln(*k*)	1/T (K^{-1})
110	**0.000720672**	-7.235326814	0.002609944
120	**0.001834821**	-6.30080839	0.002543558
125	**0.003145287**	-5.761850182	0.002511616
130	**0.005110373**	-5.276482852	0.002480466
140	**0.011962562**	-4.425973368	0.002420428

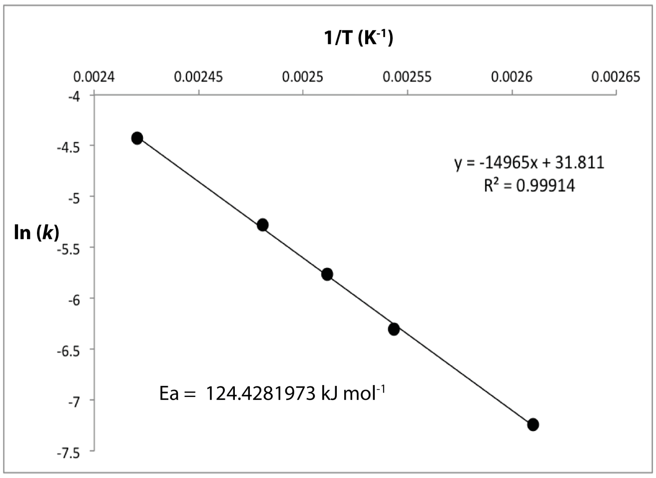

Entry 7: Thermolysis of **1a** in the presence of 4 equiv. EtOH using reverse push-out method, in-line UV analysis and OPA processing. $F_1 = 10$ mL min $^{-1}$ and $F_2 = 1$ mL min^{-1}

Temp. °C	*k*	ln(*k*)	1/T (K^{-1})
110	**0.0006236**	-7.380001173	0.002609944
115	**0.000955728**	-6.953037136	0.002576324
120	**0.001657503**	-6.402442822	0.002543558
125	**0.002795612**	-5.87970421	0.002511616
130	**0.004470768**	-5.410194983	0.002480466

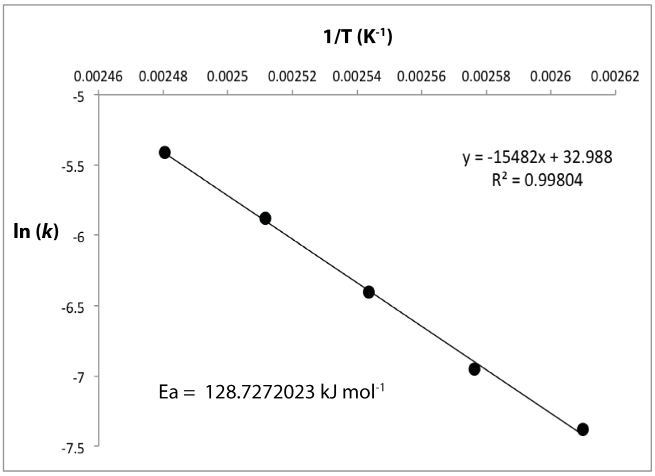

Entry 8: Thermolysis of **1a** in the presence of 4 equiv. EtOH using push-out method, in-line IR analysis and OPA processing. $F_1 = 1$ mL min $^{-1}$ and $F_2 = 2$ mL min^{-1}

Temp. °C	*k*	ln(*k*)	1/T (K^{-1})
110	**0.000658092**	-7.326165456	0.002609944
115	**0.001256256**	-6.67961957	0.002576324
120	**0.001962024**	-6.233778775	0.002543558
125	**0.002926425**	-5.833973807	0.002511616
130	**0.004801202**	-5.338889003	0.002480466

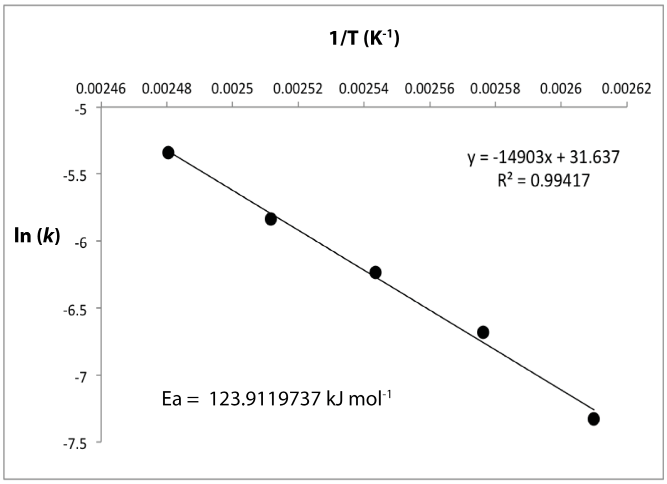

Entry 9: Thermolysis of **1a** in the presence of 4 equiv. EtOH using push-out method, in-line UV analysis and OPA processing. $F_1 = 1$ mL min $^{-1}$ and $F_2 = 2$ mL min^{-1}

Temp. °C	*k*	ln(*k*)	1/T (K^{-1})
115	**0.001029629**	-6.878556375	0.002576324
120	**0.001743752**	-6.351715927	0.002543558
125	**0.002893492**	-5.845291085	0.002511616
130	**0.004822791**	-5.334402572	0.002480466
140	**0.011302172**	-4.482760318	0.002420428

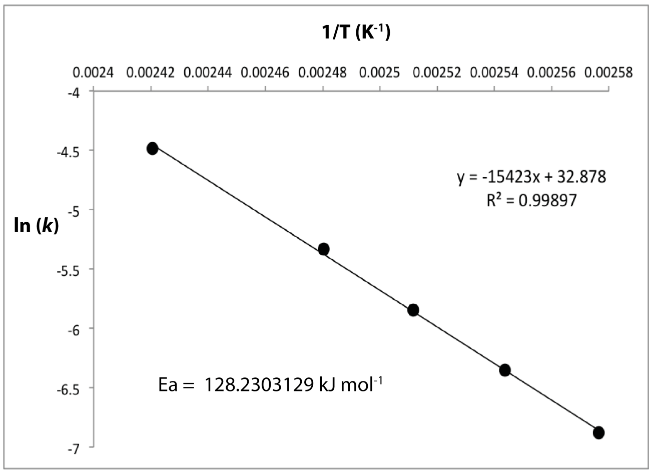

Entry 10: Thermolysis of **1a** in the presence of 4 equiv. EtOH using steady-state method and off-line ^{1}H NMR analysis.

Temp. °C	*k*	ln(*k*)	1/T (K^{-1})
110	**0.000650812**	-7.337290369	0.002609944
120	**0.001891984**	-6.270129226	0.002543558
125	**0.002966663**	-5.820317485	0.002511616
130	**0.005133186**	-5.272028777	0.002480466
140	**0.012523923**	-4.380114633	0.002420428

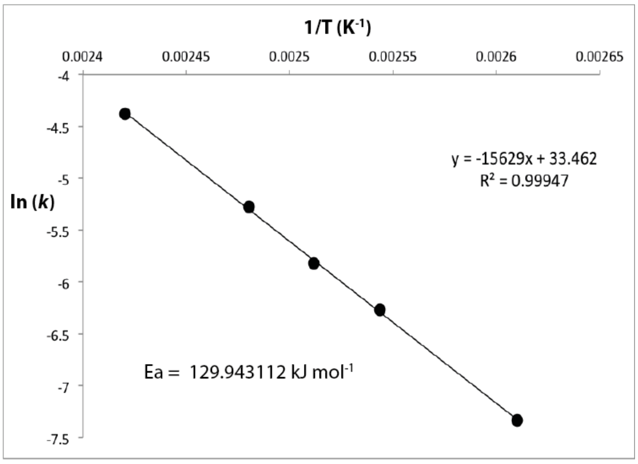

Entry 11: Thermolysis of **1a** in the presence of 4 equiv. BnOH using steady-state method and off-line ^{1}H NMR analysis.

Temp. °C	*k*	ln(*k*)	1/T (K^{-1})
110	**0.000664943**	-7.315808576	0.002609944
120	**0.00178873**	-6.326249436	0.002543558
125	**0.002847009**	-5.861486231	0.002511616
130	**0.004875351**	-5.323563212	0.002480466
135	**0.007744443**	-4.860779756	0.00245008

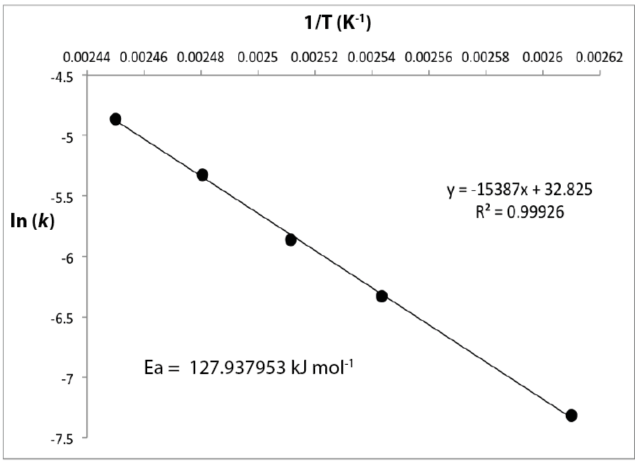

3.2 Table 2 Data

Entry 1: Thermolysis of **1b** in the presence of 4 equiv. EtOH using push-out method, in-line UV analysis and OPA processing. F_1 = 1 mL min $^{-1}$ and F_2 = 10 mL min^{-1}

Temp. °C	*k*	ln(*k*)	1/T (K^{-1})
90	**0.000235949**	-8.351893745	0.002753683
95	**0.000451353**	-7.703260275	0.002716284
100	**0.000757243**	-7.18582577	0.002679887
105	**0.001315017**	-6.633906062	0.002644453
110	**0.002190678**	-6.123544245	0.002609944
115	**0.003540051**	-5.643614193	0.002576324
120	**0.005745694**	-5.159304551	0.002543558

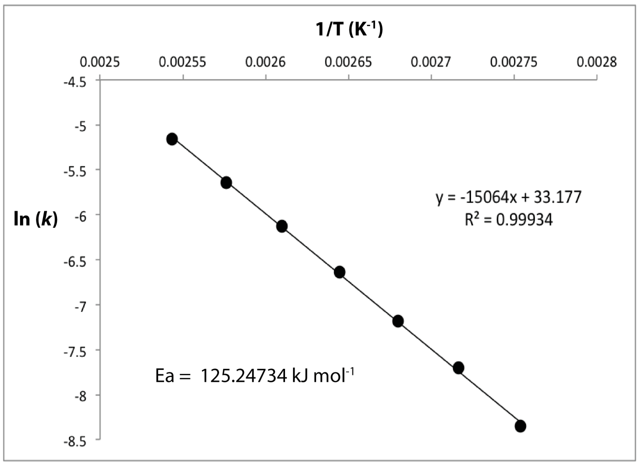

Entry 2: Thermolysis of **1b** in the presence of 4 equiv. EtOH using push-out method, in-line IR analysis and OPA processing. F_1 = 1 ml min $^{-1}$ and F_2 = 10 mL min^{-1}

Temp. °C	*k*	ln(*k*)	1/T (K^{-1})
95	**0.000482914**	-7.635672782	0.002716284
100	**0.000738087**	-7.211448701	0.002679887
105	**0.001272883**	-6.666471229	0.002644453
110	**0.002077854**	-6.176419752	0.002609944
115	**0.003547972**	-5.641379045	0.002576324
120	**0.005840732**	-5.142899118	0.002543558

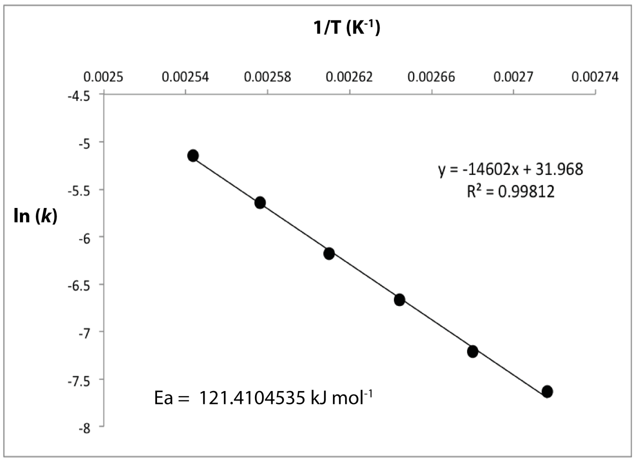

Entry 3: Thermolysis of **1b** in the presence of 4 equiv. EtOH using steady-state method, in-line UV analysis and OPA processing.

Temp. °C	*k*	ln(*k*)	1/T (K^{-1})
100	**0.000799534**	-7.131481027	0.002679887
105	**0.001312299**	-6.6359748	0.002644453
110	**0.002298925**	-6.075313502	0.002609944
115	**0.003703033**	-5.598602973	0.002576324
120	**0.006155691**	-5.090378247	0.002543558

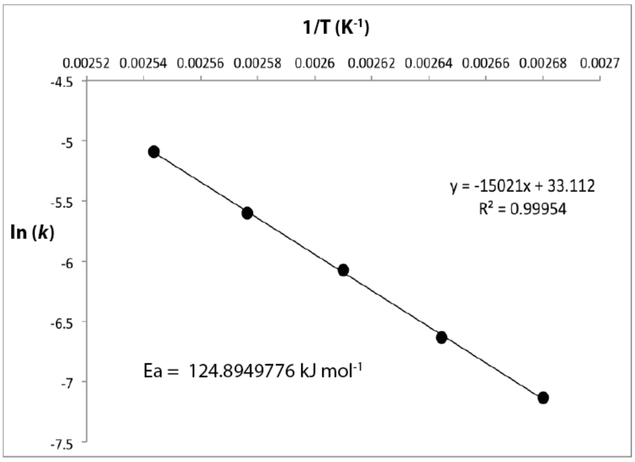

Entry 4: Thermolysis of **1b** in the presence of 4 equiv. BnOH using steady-state method and off-line ^{1}H NMR analysis.

Temp. °C	*k*	ln(*k*)	1/T (K^{-1})
100	**0.000792559**	-7.140243736	0.002679887
105	**0.001237786**	-6.694430877	0.002644453
110	**0.002330798**	-6.061544518	0.002609944
115	**0.003288001**	-5.717475544	0.002576324
120	**0.006263254**	-5.073055398	0.002543558

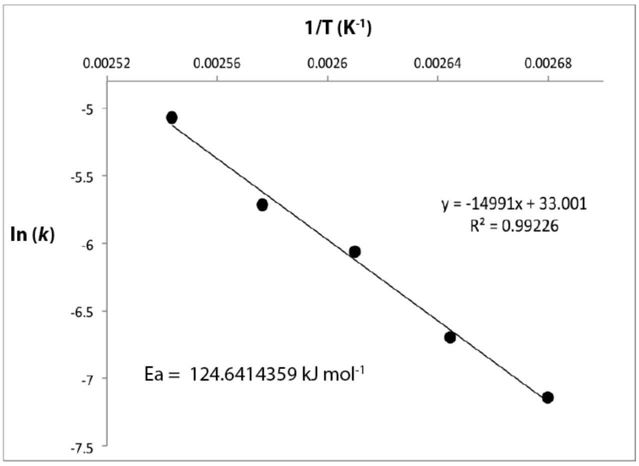

Entry 5: Thermolysis of **1c** in the presence of 4 equiv. EtOH using push-out method, in-line UV analysis and OPA processing. $F_1 = 1$ mL min $^{-1}$ and $F_2 = 10$ mL min^{-1}

Temp. °C	*k*	ln(*k*)	1/T (K^{-1})
85	**0.001657298**	-6.402566921	0.002792126
90	**0.002778499**	-5.885844536	0.002753683
95	**0.004707618**	-5.358573137	0.002716284
100	**0.007551304**	-4.886035037	0.002679887
105	**0.011486105**	-4.466617238	0.002644453
110	**0.017175729**	-4.06425797	0.002609944

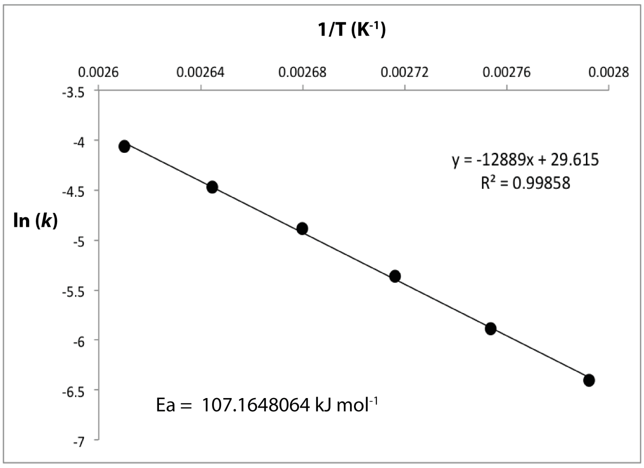

Entry 6: Thermolysis of **1c** in the presence of 4 equiv. EtOH using push-out method, in-line IR analysis and OPA processing. $F_1 = 1$ mL min $^{-1}$ and $F_2 = 10$ mL min^{-1}

Temp. °C	*k*	ln(*k*)	1/T (K^{-1})
90	**0.002653613**	-5.931833014	0.002753683
95	**0.004515082**	-5.400332022	0.002716284
100	**0.007151931**	-4.940372954	0.002679887
105	**0.011110539**	-4.49986112	0.002644453

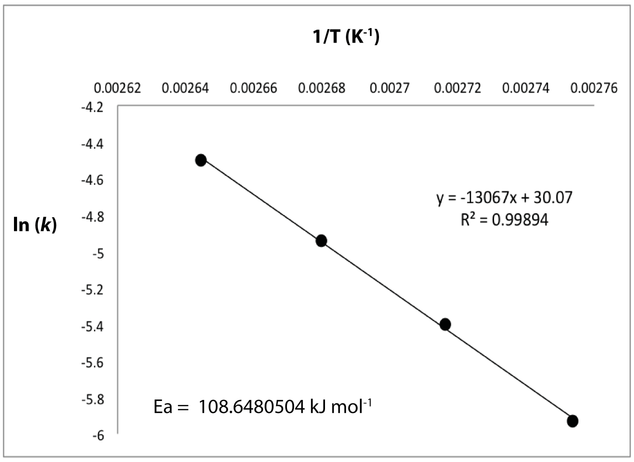

Entry 7: Thermolysis of **1d** in the presence of 4 equiv. EtOH using push-out method, in-line UV analysis and OPA processing. $F_1 = 1$ mL min $^{-1}$ and $F_2 = 10$ mL min^{-1}

Temp. °C	*k*	ln(*k*)	1/T (K^{-1})
100	**0.000587258**	-7.440046666	0.002679887
105	**0.000940204**	-6.969413897	0.002644453
110	**0.001587826**	-6.445389647	0.002609944
115	**0.002680919**	-5.921595548	0.002576324
120	**0.004544167**	-5.393910956	0.002543558
125	**0.007797548**	-4.853946008	0.002511616

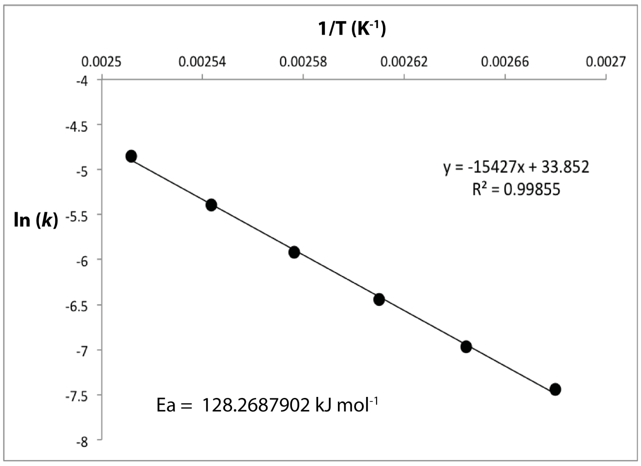

Entry 8: Thermolysis of **1d** in the presence of 4 equiv. EtOH using push-out method, in-line IR analysis and OPA processing. $F_1 = 1$ mL min $^{-1}$ and $F_2 = 10$ mL min^{-1}

Temp. °C	*k*	ln(*k*)	1/T (K^{-1})
100	**0.000559079**	-7.489220301	0.002679887
105	**0.001062288**	-6.84733043	0.002644453
110	**0.001821606**	-6.308036506	0.002609944
115	**0.00290625**	-5.840891657	0.002576324
125	**0.007468588**	-4.89704927	0.002511616

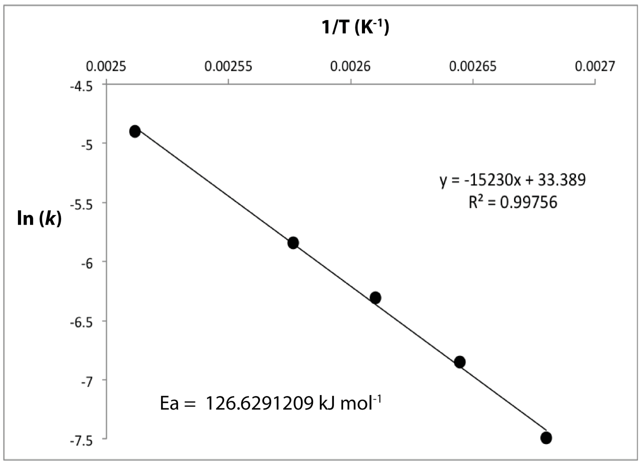

Entry 9: Thermolysis of **1d** in the presence of 4 equiv. EtOH using push-out method and off-line ^{1}H NMR analysis. $F_1 = 1$ mL min $^{-1}$ and $F_2 = 10$ mL min^{-1}

Temp. °C	*k*	ln(*k*)	1/T (K^{-1})
100	**0.000549312**	-7.506844753	0.002679887
105	**0.000949227**	-6.959863109	0.002644453
110	**0.001618969**	-6.425965795	0.002609944
115	**0.002595547**	-5.95395782	0.002576324
125	**0.007418929**	-4.903720599	0.002511616

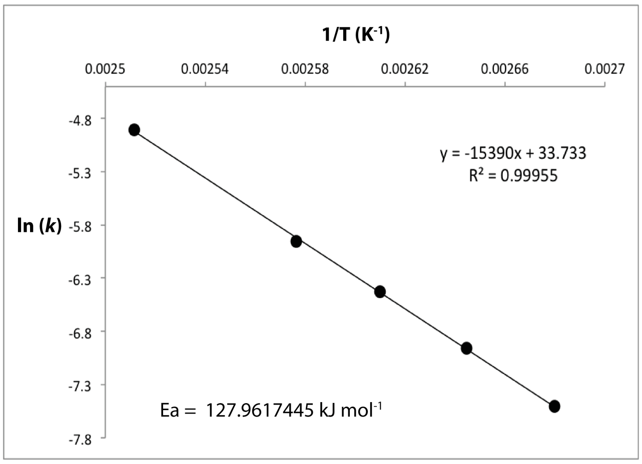

Entry 10: Thermolysis of **1e** in the presence of 4 equiv. EtOH using push-out method, in-line UV analysis and OPA processing. $F_1 = 1$ mL min $^{-1}$ and $F_2 = 10$ mL min^{-1}

Temp. °C	*k*	ln(*k*)	1/T (K^{-1})
105	**0.000317165**	-8.056088364	0.002644453
110	**0.000549577**	-7.506362469	0.002609944
115	**0.000934674**	-6.975313126	0.002576324
120	**0.001564908**	-6.459928409	0.002543558
125	**0.002577148**	-5.961072079	0.002511616
130	**0.004044506**	-5.510395867	0.002480466

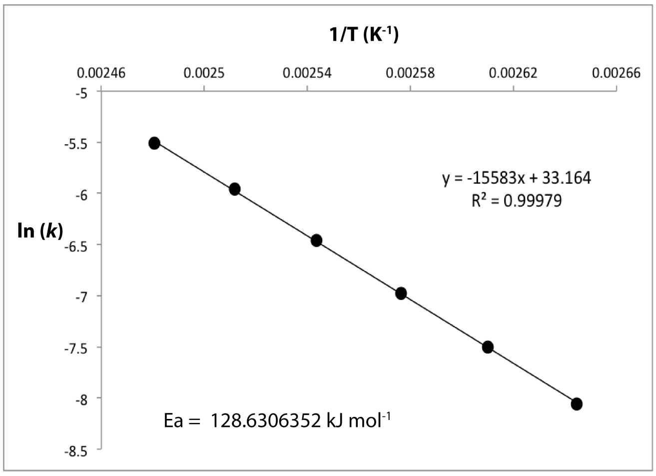

Entry 11: Thermolysis of **1f** in the presence of 4 equiv. EtOH using push-out method, in-line UV analysis and OPA processing. $F_1 = 1$ mL min $^{-1}$ and $F_2 = 10$ mL min^{-1}

Temp. °C	*k*	ln(*k*)	1/T (K^{-1})
110	**0.000436225**	-7.737353348	0.002609944
115	**0.000755304**	-7.188390581	0.002576324
120	**0.001300208**	-6.645230969	0.002543558
130	**0.003623828**	-5.620224358	0.002480466

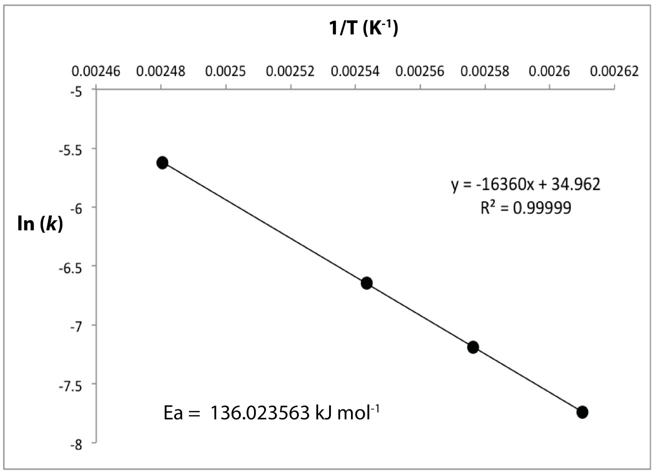

Entry 12: Thermolysis of **1g** in the presence of 4 equiv. EtOH using push-out method, in-line UV analysis and OPA processing. $F_1 = 1$ mL min $^{-1}$ and $F_2 = 10$ mL min^{-1}

Temp. °C	*k*	ln(*k*)	1/T (K^{-1})
100	**0.000573185**	-7.464301215	0.002679887
105	**0.000909735**	-7.002357313	0.002644453
110	**0.001525452**	-6.485464637	0.002609944
115	**0.002472934**	-6.002350147	0.002576324
120	**0.004149356**	-5.484802097	0.002543558

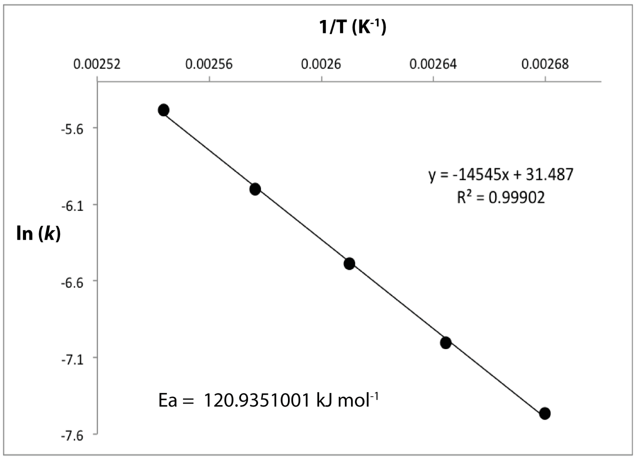

Entry 13: Thermolysis of **1h** in the presence of 4 equiv. EtOH using push-out method, in-line UV analysis and OPA processing. $F_1 = 1$ mL min $^{-1}$ and $F_2 = 10$ mL min^{-1}

Temp. °C	*k*	ln(*k*)	1/T (K^{-1})
90	**0.000369181**	-7.904224179	0.002753683
95	**0.000605304**	-7.409779526	0.002716284
100	**0.001052721**	-6.856377076	0.002679887
105	**0.001720652**	-6.365052182	0.002644453
110	**0.002992631**	-5.811602273	0.002609944
115	**0.004949794**	-5.30840922	0.002576324

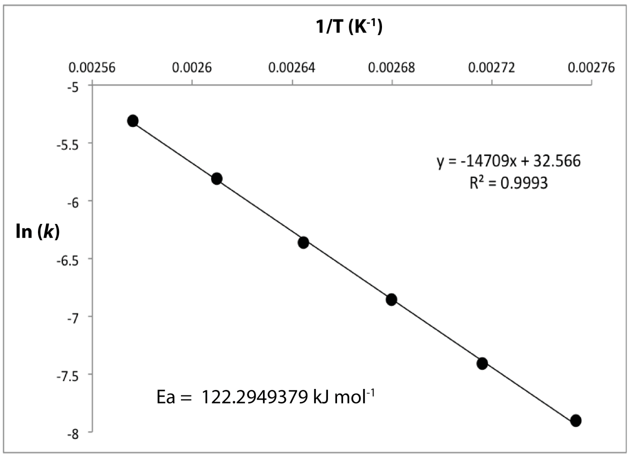

Entry 14: Thermolysis of **1i** in the presence of 4 equiv. EtOH using push-out method, in-line UV analysis and OPA processing. $F_1 = 1$ mL min $^{-1}$ and $F_2 = 10$ mL min^{-1}

Temp. °C	*k*	ln(*k*)	1/T (K^{-1})
100	**0.000206094**	-8.487176355	0.002679887
105	**0.000343122**	-7.977424319	0.002644453
110	**0.000591477**	-7.432887072	0.002609944
115	**0.00096223**	-6.946257411	0.002576324
120	**0.001602055**	-6.436468292	0.002543558
130	**0.003978796**	-5.526776097	0.002480466

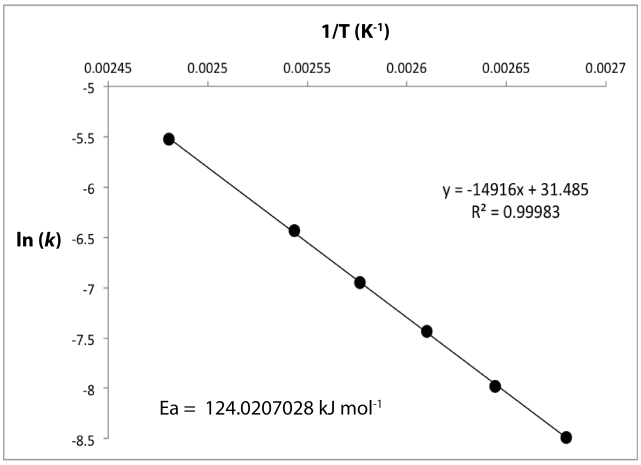

4. Off-Line ^{1}H NMR Analysis

4.1 General Methods

^{1}H NMR spectra of crude samples were recorded following solvent removal *in vacuo* from fractions collected under steady-state conditions as described in section 1.3. All ^{1}H NMR spectra were obtained on a AV300 or DPX400 MHz spectrometer in $CDCl_3$. ^{1}H chemical shifts are reported as values in ppm referenced to residual solvent. Individual rate constants for thermal cycloreversion of **1a**, **1b** and **1d** were determined from the peak integrals indicated in section 4.2 below. In plotting ln([**1**]/[**1**]$_0$) it is assumed that [**1** + **4** + **4**$_{\text{tautomer}}$] ≡ [**1**]$_0$ where **4** is the β-keto ester product of ketene trapping by EtOH or BnOH, since no evidence of competing condensation of ketenes **3a**/**b**/**d** with the ketone product of thermolysis, or of competing [4+2] self-cycloaddition of **3a**/**b**/**d** was observed. Where the ketone product **2** is non-volatile, [**1** + **2**] ≡ [**1**]$_0$. Activation energies for thermolysis of **1a** **1b** and **1d** calculated from the rate constants reported in section 4.2 below, are given in sections 3.1 and 3.2 respectively.

4.2 Rate Constant Data

4.2.1 Table 1, Entry 10: Thermolysis of **1a** in the presence of 4 equiv. EtOH under steady-state conditions.

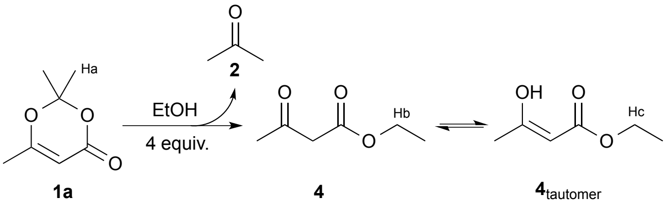

Peaks used in calculation of [**1a**]/[**1a** + **4** + **4**$_{\text{tautomer}}$]: δ = 1.69 (6H, s, Ha), 4.20 (2H, q, J = 7.0 Hz, Hb), 4.19 (2H, q, J = 7.0 Hz, Hc) ppm (300MHz).

Sample data collected from experiments carried out at 130 °C is shown in Figure S4.1.

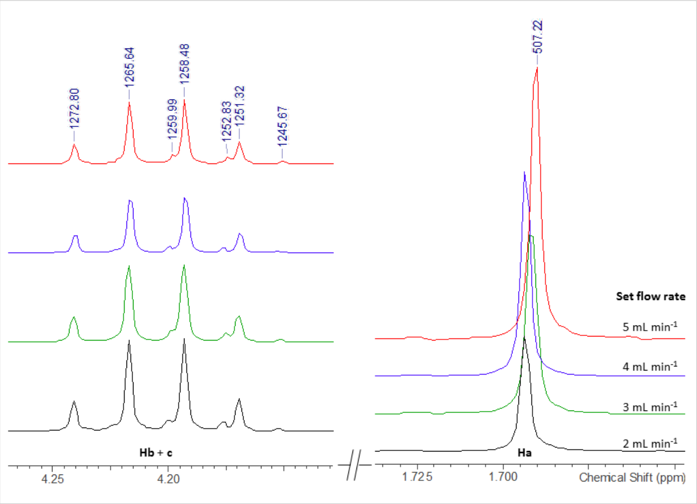

Figure S4.1

Reaction temperature = 110 °C			
Set flow (mL min^{-1})	Effective flow (mL min^{-1})	Reaction time (sec.)	ln([**1a**]/[**1a** + **4** + **4**$_{\text{tautomer}}$])
7	7.78638	75.20824825	-0.029558802
5	5.5617	105.2915475	-0.048790164
4	4.44936	131.6144344	-0.062974799
3	3.33702	175.4859126	-0.09531018

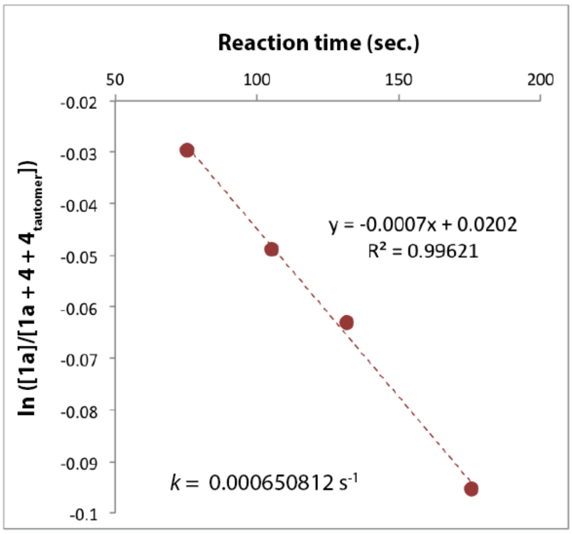

Reaction temperature = 120 °C			
Set flow (mL min^{-1})	Effective flow (mL min^{-1})	Reaction time (sec.)	ln([**1a**]/[**1a** + **4** + **4**$_{\text{tautomer}}$])
7	7.88228	74.2932248	-0.131028262
5	5.6302	104.0105147	-0.186479567
4	4.50416	130.0131434	-0.235072122
3	3.37812	173.3508579	-0.318453731

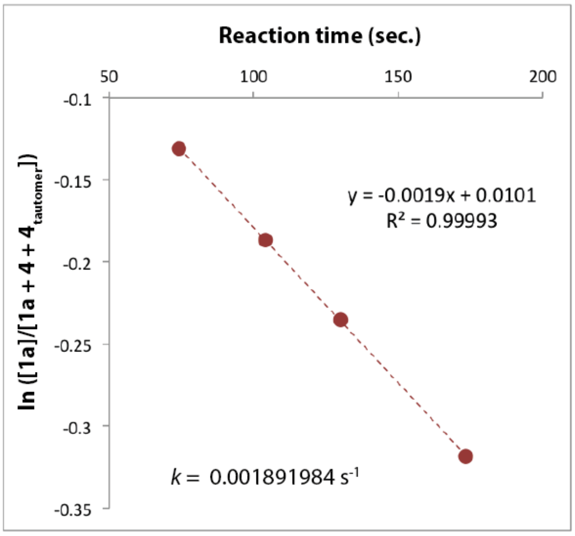

Reaction temperature = 125 °C			
Set flow (mL min^{-1})	Effective flow (mL min^{-1})	Reaction time (sec.)	ln([**1a**]/[**1a** + **4** + **4**$_{\text{tautomer}}$])
7	7.93023	73.84401209	-0.207014169
5	5.66445	103.3816169	-0.296394013
4	4.53156	129.2270212	-0.381855242
3	3.39867	172.3026949	-0.497740384

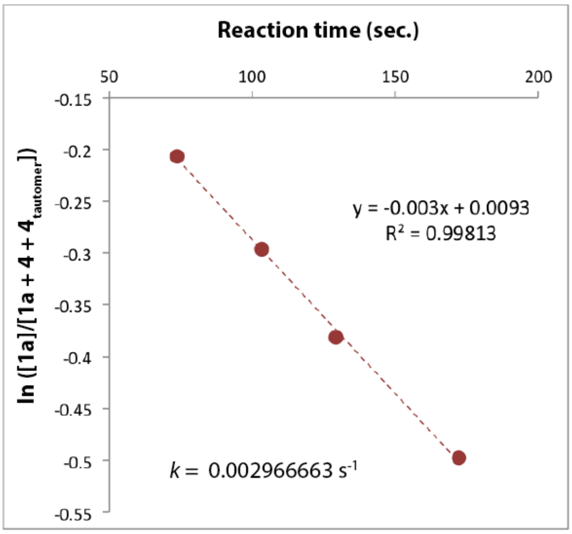

Reaction temperature = 130 °C			
Set flow (mL min^{-1})	Effective flow (mL min^{-1})	Reaction time (sec.)	ln([**1a**]/[**1a** + **4** + **4**$_{\text{tautomer}}$])
5	5.6987	102.7602787	-0.476234179
4	4.55896	128.4503483	-0.612479277
3	3.41922	171.2671311	-0.819779831
2	2.27948	256.9006967	-1.269760545

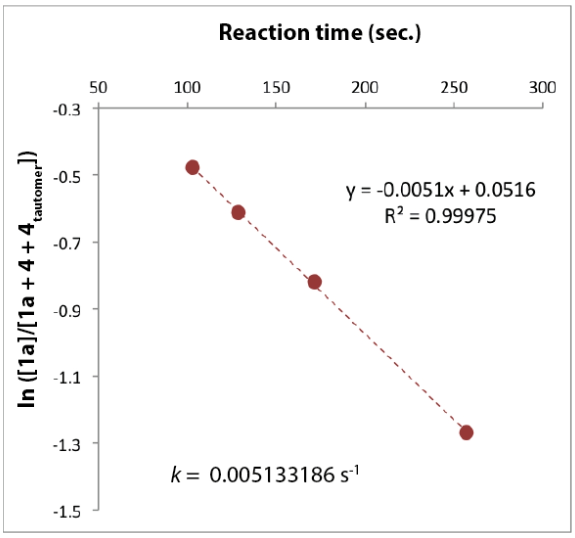

Reaction temperature = 140 °C			
Set flow (mL min^{-1})	Effective flow (mL min^{-1})	Reaction time (sec.)	$\ln([\mathbf{1a}]/[\mathbf{1a} + \mathbf{4} + \mathbf{4}_{tautomer}])$
5	5.7672	101.539742	-1.239822457
4	4.61376	126.9246775	-1.561297537
3	3.46032	169.2329033	-2.088153482

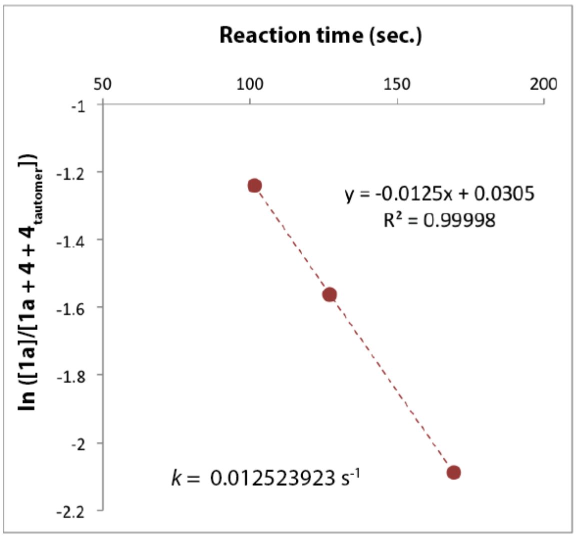

4.2.2 Table 1, Entry 11: Thermolysis of **1a** in the presence of 4 equiv. BnOH under steady-state conditions.

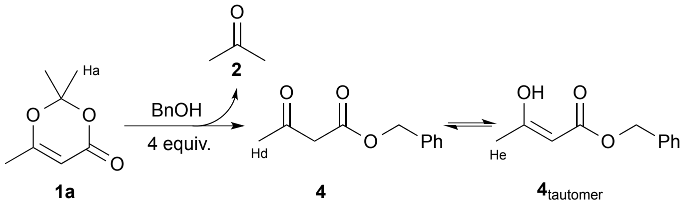

Peaks used in calculation of [**1a**]/[**1a** + **4** + **4**$_{tautomer}$]: δ = 1.69 (6H, s, Ha), 2.20 (3H, s, Hd), 1.99 (3H, s, He) ppm (400 MHz).

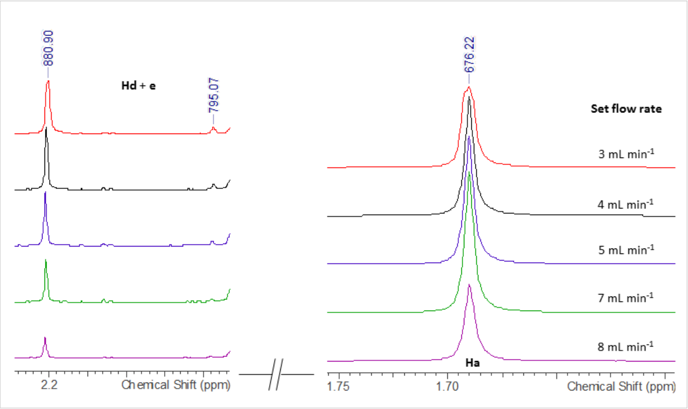

Sample data collected from experiments carried out at 125 °C is shown in Figure S4.2.

Scheme S4.2

Reaction temperature = 110 °C			
Set flow (mL min^{-1})	Effective flow (mL min^{-1})	Reaction time (sec.)	$\ln([\mathbf{1a}]/[\mathbf{1a} + \mathbf{4} + \mathbf{4}_{tautomer}])$
8	8.89872	65.80721722	-0.032789823
7	7.78638	75.20824825	-0.039220713
5	5.5617	105.2915475	-0.055119299
4	4.44936	131.6144344	-0.070769071
3	3.33702	175.4859126	-0.107358518

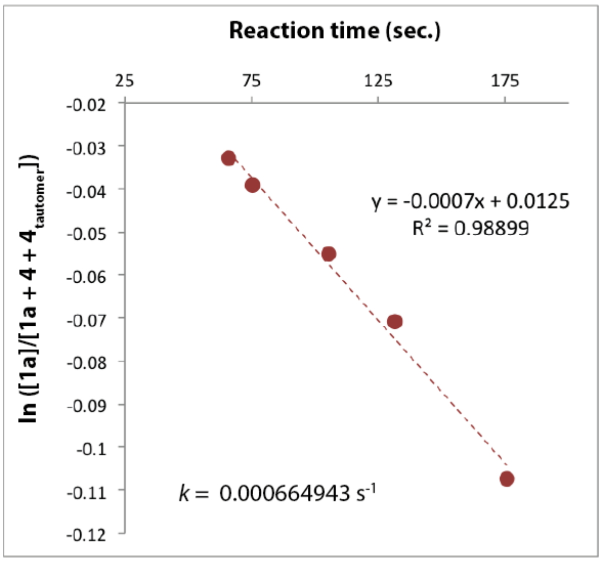

Reaction temperature = 120 °C			
Set flow (mL min^{-1})	Effective flow (mL min^{-1})	Reaction time (sec.)	ln([**1a**]/[**1a** + **4** + **4**$_{tautomer}$])
8	9.00832	65.0065717	-0.09531018
7	7.88228	74.2932248	-0.110348057
5	5.6302	104.0105147	-0.162685582
4	4.50416	130.0131434	-0.220473323
3	3.37812	173.3508579	-0.285178942

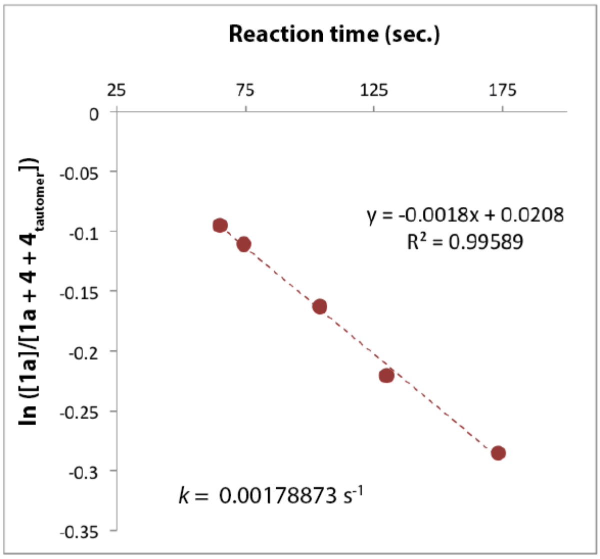

Reaction temperature = 125 °C			
Set flow (mL min^{-1})	Effective flow (mL min^{-1})	Reaction time (sec.)	ln([**1a**]/[**1a** + **4** + **4**$_{tautomer}$])
8	9.06312	64.61351058	-0.162685582
7	7.93023	73.84401209	-0.182321557
5	5.66445	103.3816169	-0.267479365
4	4.53156	129.2270212	-0.331698958
3	3.39867	172.3026949	-0.470003629

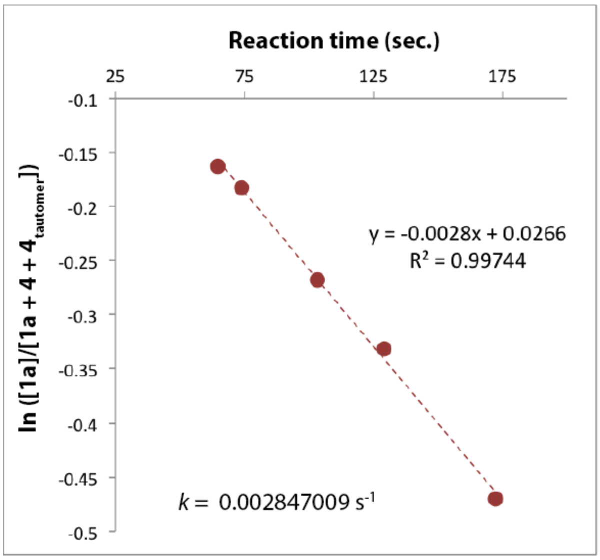

Reaction temperature = 130 °C			
Set flow (mL min^{-1})	Effective flow (mL min^{-1})	Reaction time (sec.)	ln([**1a**]/[**1a** + **4** + **4**$_{tautomer}$])
8	9.11792	64.22517416	-0.257222865
7	7.97818	73.40019904	-0.312374685
5	5.6987	102.7602787	-0.440403159
4	4.55896	128.4503483	-0.576613364
3	3.41922	171.2671311	-0.782378314

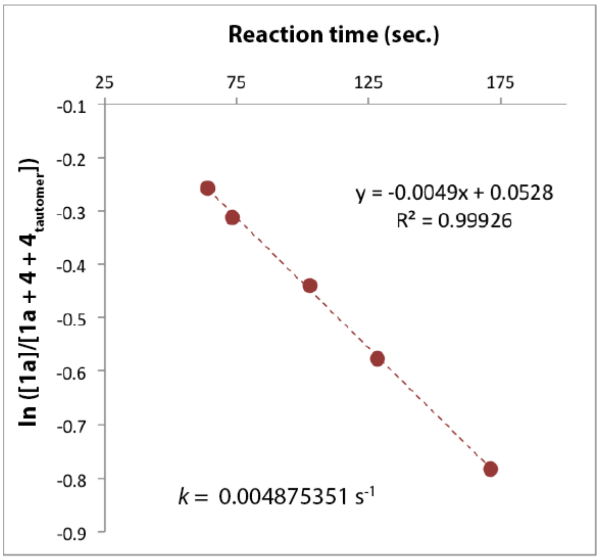

Reaction temperature = 135 °C			
Set flow (mL min^{-1})	Effective flow (mL min^{-1})	Reaction time (sec.)	ln([**1a**]/[**1a** + **4** + $\mathbf{4}_{tautomer}$])
8	9.17272	63.84147777	-0.429615568
7	8.02613	72.96168888	-0.500775288
5	5.73295	102.1463644	-0.75612198
4	4.58636	127.6829555	-0.90016135
3	3.43977	170.2439407	-1.264126727

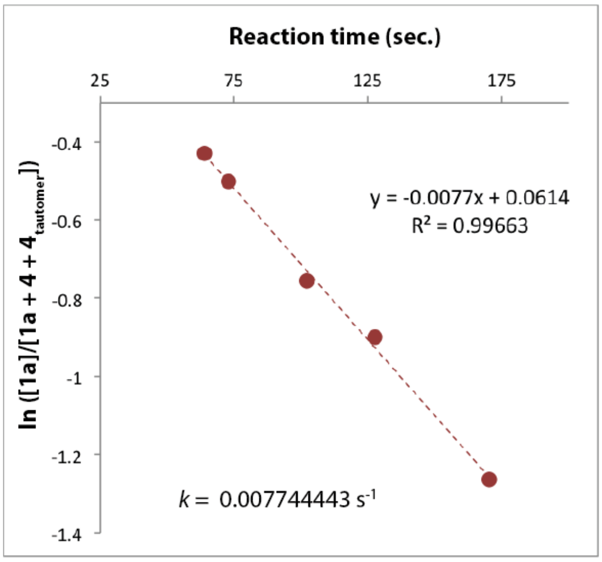

4.2.3 Table 2, Entry 4: Thermolysis of **1b** in the presence of 4 equiv. BnOH under steady-state conditions.

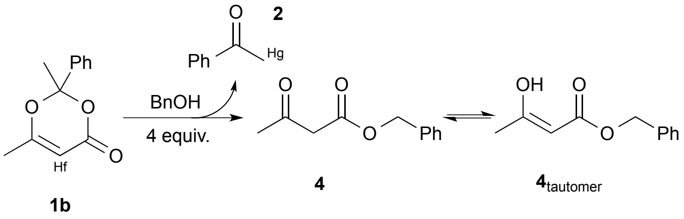

Peaks used in calculation of [**1b**]/[**1b** + **2**]: δ = 5.16 (1H, q, J = 0.7 Hz, Hf), 2.62 (3H, s, Hg) ppm (400 MHz).

Sample data collected from experiments carried out at 105 °C is shown in Figure S4.3.

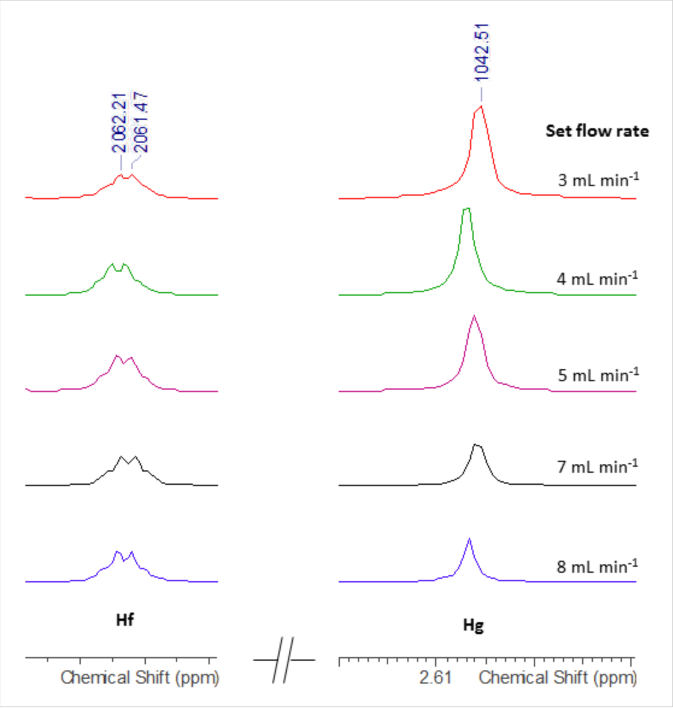

Scheme S4.3

Reaction temperature = 100 °C			
Set flow (mL min^{-1})	Effective flow (mL min^{-1})	Reaction time (sec.)	ln([**1b**]/[**1b** + **2**])
8	8.78912	66.62783077	-0.046025822
7	7.69048	76.14609231	-0.049480057
5	5.4932	106.6045292	-0.076540077
4	4.39456	133.2556615	-0.097374164
3	3.29592	177.6742154	-0.132171773

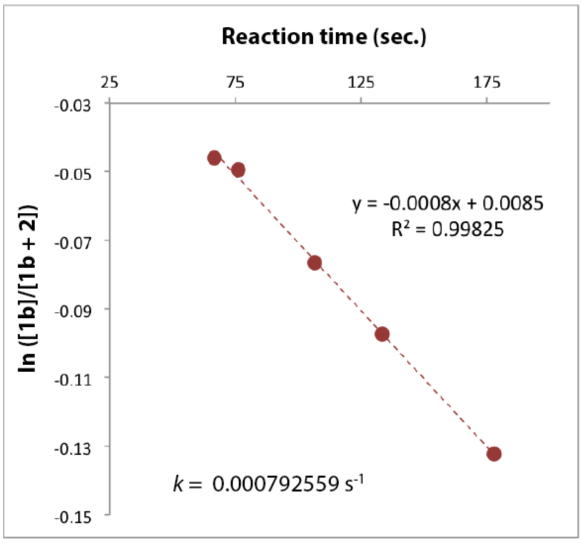

Reaction temperature = 105 °C			
Set flow (mL min^{-1})	Effective flow (mL min^{-1})	Reaction time (sec.)	ln([**1b**]/[**1b** + **2**])
8	8.84392	66.21498159	-0.067822596
7	7.73843	75.67426468	-0.078692269
5	5.52745	105.9439705	-0.120901773
4	4.42196	132.4299632	-0.171422266
3	3.31647	176.5732842	-0.197298011

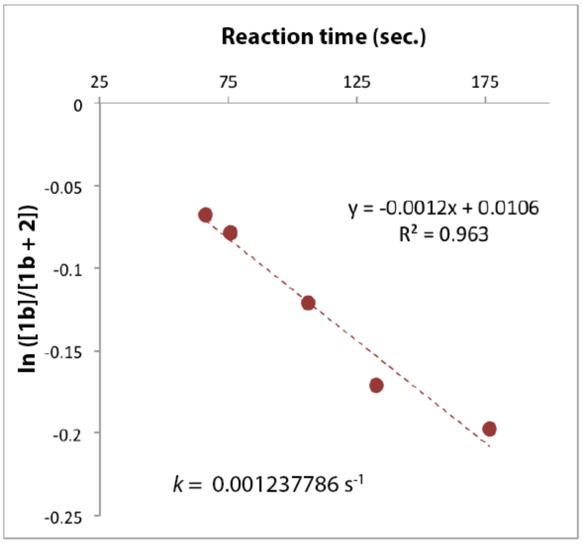

Reaction temperature = 110 °C			
Set flow (mL min^{-1})	Effective flow (mL min^{-1})	Reaction time (sec.)	ln([**1b**]/[**1b** + **2**])
8	8.89872	65.80721722	-0.110900696
7	7.78638	75.20824825	-0.159630146
5	5.5617	105.2915475	-0.2135741
4	4.44936	131.6144344	-0.27510329

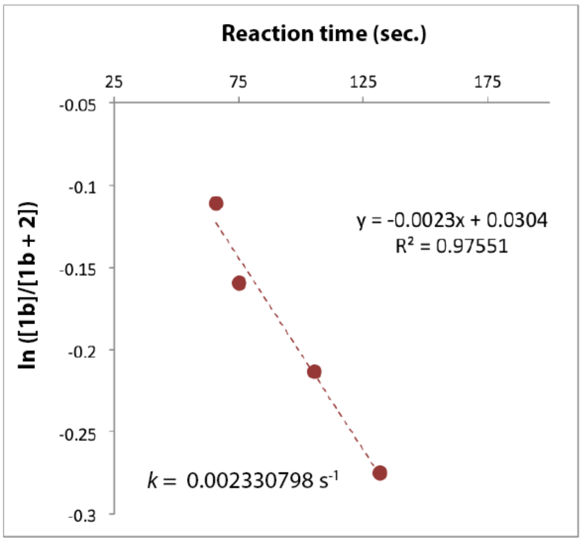

Reaction temperature = 115 °C			
Set flow (mL min^{-1})	Effective flow (mL min^{-1})	Reaction time (sec.)	ln([**1b**]/[**1b** + **2**])
8	8.95352	65.40444429	-0.199441439
7	7.83433	74.74793633	-0.233288
5	5.59595	104.6471109	-0.316669609
4	4.47676	130.8088886	-0.415293197
3	3.35757	174.4118514	-0.558327958

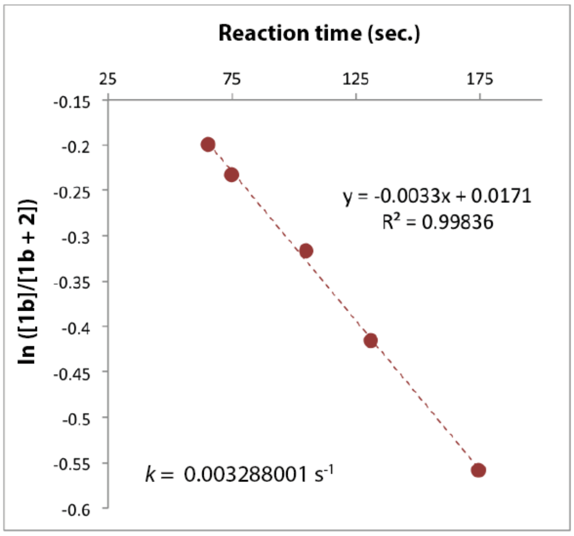

Reaction temperature = 120 °C			
Set flow (mL min^{-1})	Effective flow (mL min^{-1})	Reaction time (sec.)	ln([**1b**]/[**1b** + **2**])
8	9.00832	65.0065717	-0.29951653
7	7.88228	74.2932248	-0.399155939
5	5.6302	104.0105147	-0.537623817
4	4.50416	130.0131434	-0.701550591
3	3.37812	173.3508579	-1.001946176

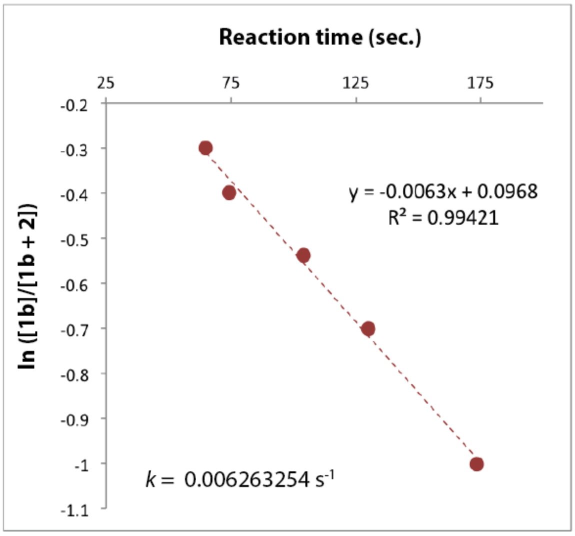

4.2.4 Table 2, Entry 9: Thermolysis of **1d** in the presence of 4 equiv. EtOH under push-out conditions where F_1 = 1 mL min $^{-1}$ and F_2 = 10 mL min^{-1}.

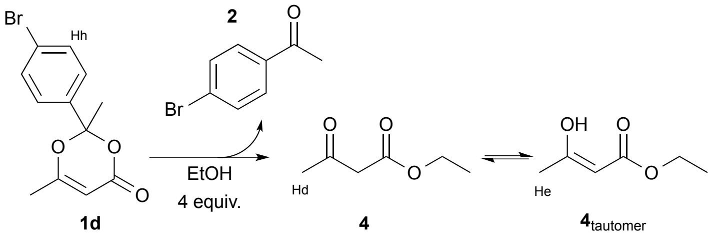

Peaks used in calculation of [**1d**]/[**1d** + **4** + **4**$_{\text{tautomer}}$]: δ = 7.51 (2H, d, J = 8.8 Hz, Hh), 2.20 (3H, s, Hd), 1.99 (3H, s, He) ppm (400 MHz).

Sample data collected from experiments carried out at 115 °C is shown in Figure S4.4.

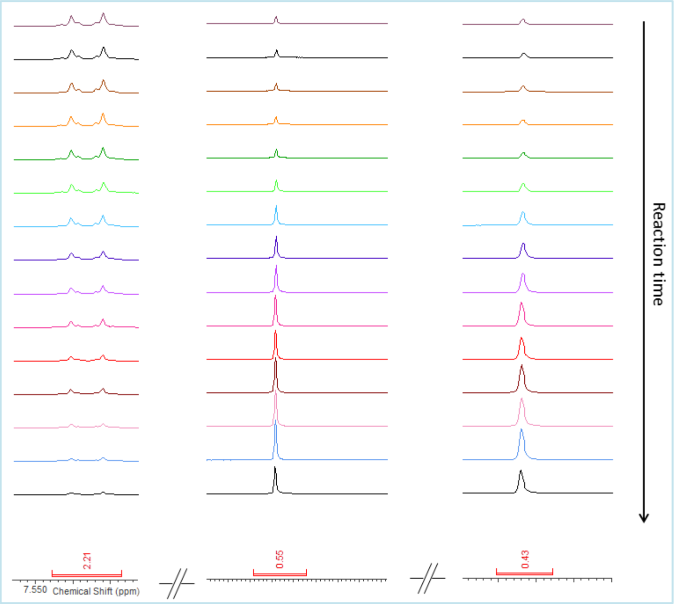

Scheme S4.4

Reaction temperature = 100 °C	
Reaction time (sec.)	ln([**1d**]/[**1d** + **4** + $\mathbf{4}_{\text{tautomer}}$])
373.8564322	-0.249144053
332.942211	-0.228462713
292.0279898	-0.199783384
251.1137685	-0.178721941
210.1995473	-0.152762755
169.2853261	-0.135472513
128.3711049	-0.113574114
87.45688367	-0.092781733

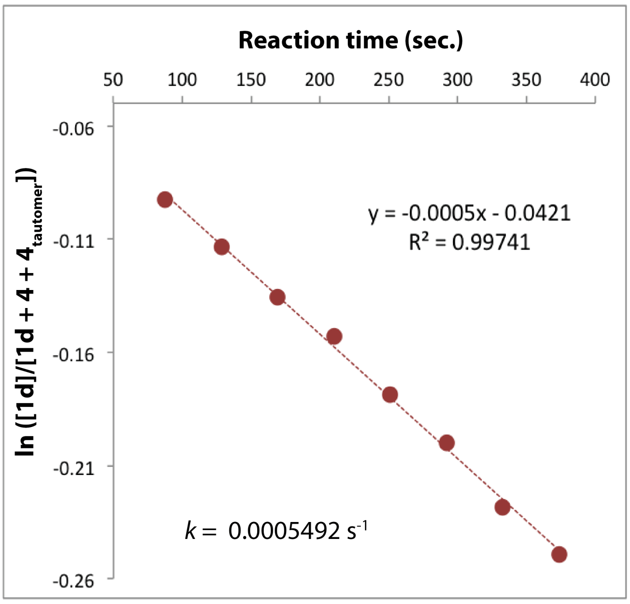

Reaction temperature = 105 °C	
Reaction time (sec.)	ln([**1d**]/[**1d** + **4** + $\mathbf{4}_{\text{tautomer}}$])
327.8211517	-0.37491044
287.1604492	-0.333116529
246.4997467	-0.298044859
205.8390442	-0.25386545
165.1783417	-0.216807733
124.5176392	-0.183745045
83.85693675	-0.141339117

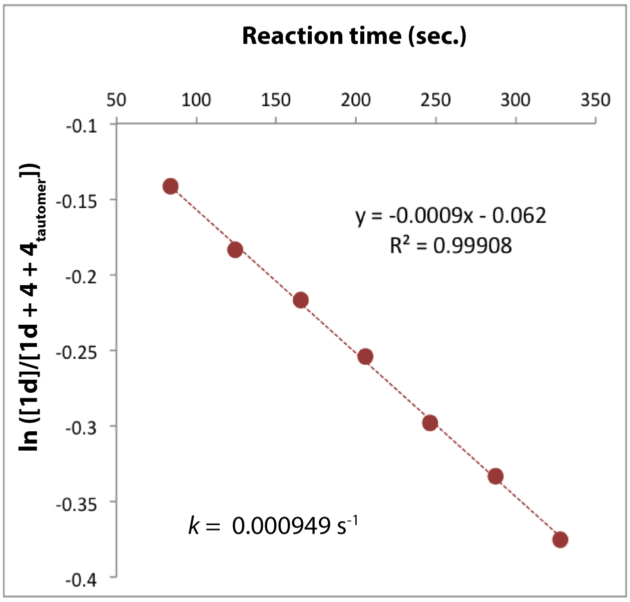

Reaction temperature = 110 °C	
Reaction time (sec.)	ln([**1d**]/[**1d** + **4** + $\mathbf{4}_{\text{tautomer}}$])
322.8005973	-0.635446467
282.3902911	-0.575067892
241.9799849	-0.505175891
201.5696787	-0.440797019
161.1593725	-0.381680203
120.7490663	-0.317428466
80.33876009	-0.24449214
39.92845389	-0.179364963

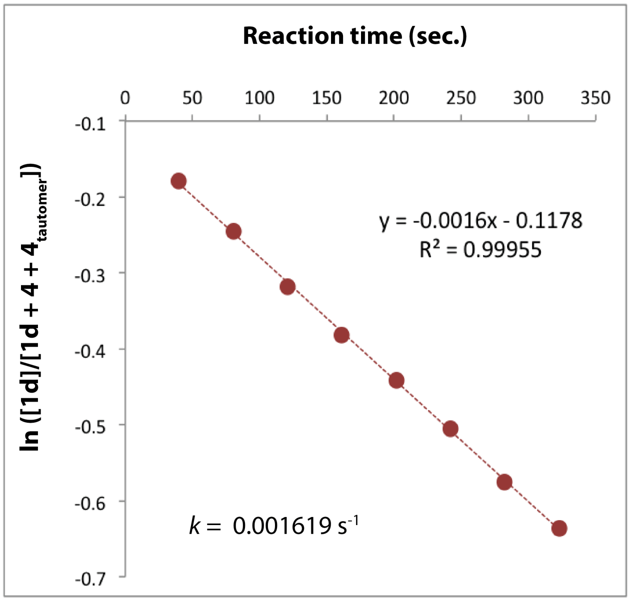

Reaction temperature = 115 °C	
Reaction time (sec.)	$\ln([\mathbf{1d}]/[\mathbf{1d} + \mathbf{4} + \mathbf{4}_{\mathrm{tautomer}}])$
277.7150442	-0.901691932
237.5520692	-0.774188391
197.3890942	-0.671625014
157.2261192	-0.565446708
117.0631442	-0.463927941
76.90016917	-0.362114667

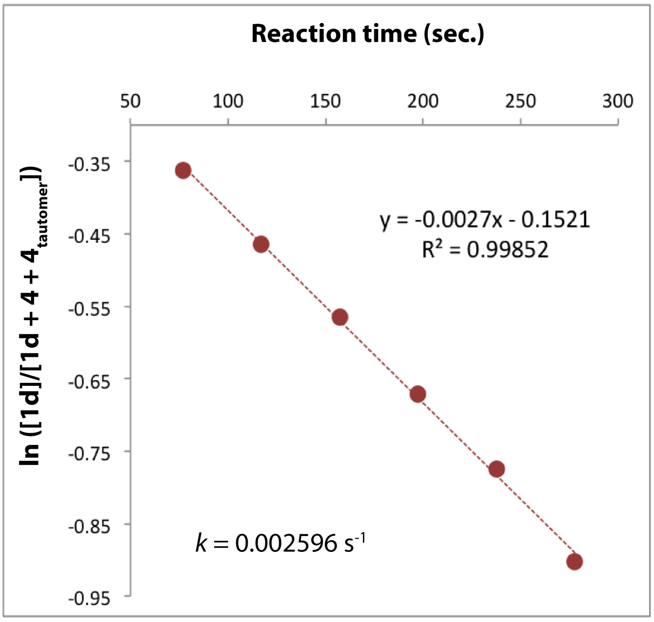

Reaction temperature = 125 °C	
Reaction time (sec.)	$\ln([\mathbf{1d}]/[\mathbf{1d} + \mathbf{4} + \mathbf{4}_{\mathrm{tautomer}}])$
268.6397799	-2.297367567
228.9624944	-1.912239482
189.2852088	-1.646903854
149.6079233	-1.39976906
109.9306378	-1.056511615
70.25335225	-0.783491672
30.57606673	-0.499275928

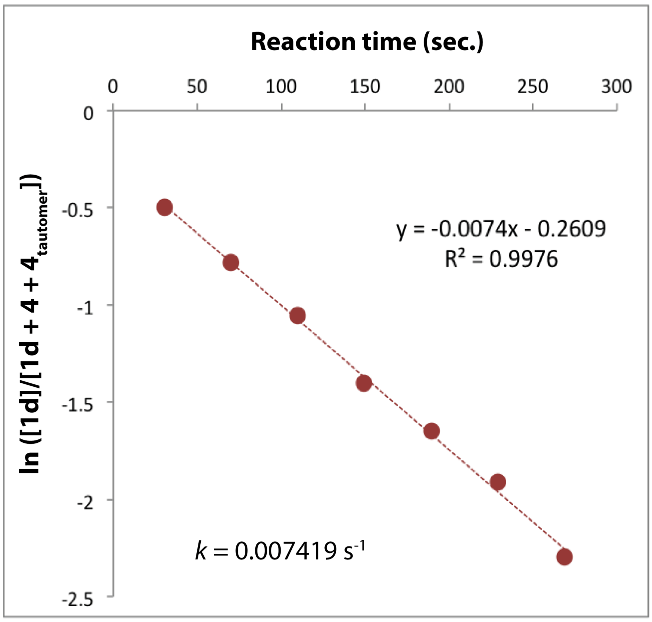

5. Alcohol Stoichiometry Experiments

Solutions of 2,2,6-trimethyl-4*H*-1,3-dioxin-4-one (**1a**) ([**1a**] = 0.3 mM) and ethanol (0.5, 1.0, 2.0 or 4.0 equiv.) in dry acetonitrile (100 mL) were prepared. In each case, steady-state kinetic study and sample collection was carried out at 120 °C according to the general method described in section 1.3. Off-line ^{1}H NMR analysis was carried out according to the general method described in section 4, assuming $[\mathbf{1} + \mathbf{4} + \mathbf{4}_{\mathrm{tautomer}}] \equiv [\mathbf{1}]_0$. First-order rate constants for thermolysis of **1a** were calculated from identical peak analysis to that described in section 4.2.1, *i.e.* peaks used in calculation of $[\mathbf{1a}]/[\mathbf{1a} + \mathbf{4} + \mathbf{4}_{\mathrm{tautomer}}]$: δ = 1.69 (6H, s, Ha), 4.20 (2H, q, J = 7.0 Hz, Hb), 4.19 (2H, q, J = 7.0 Hz, Hc) ppm.

0.5 Equiv. EtOH			
Set flow (mL min^{-1})	Effective flow (mL min^{-1})	Reaction time (sec.)	$\ln([\mathbf{1a}]/[\mathbf{1a} + \mathbf{4} + \mathbf{4}_{\mathrm{tautomer}}])$
9	10.13436	57.78361929	-0.062974799
7	7.88228	74.2932248	-0.086177696
5	5.6302	104.0105147	-0.126632651
3	3.37812	173.3508579	-0.21913553
2	2.25208	260.0262868	-0.347129531

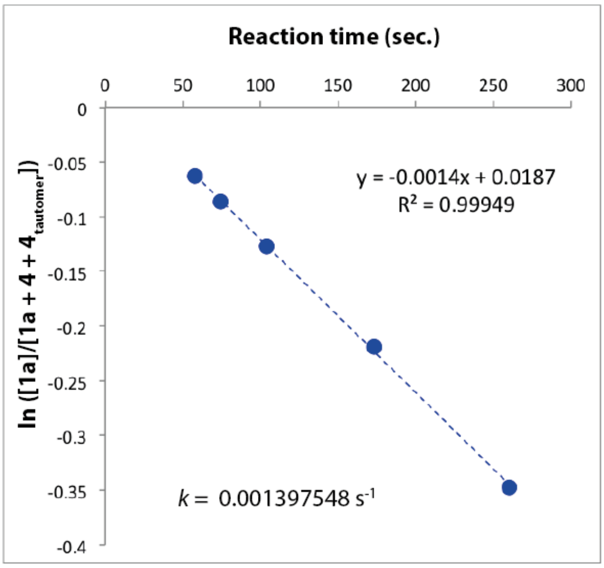

1.0 Equiv. EtOH			
Set flow (mL min^{-1})	Effective flow (mL min^{-1})	Reaction time (sec.)	$\ln([\mathbf{1a}]/[\mathbf{1a} + \mathbf{4} + \mathbf{4}_{\mathrm{tautomer}}])$
9	10.13436	57.78361929	-0.09531018
7	7.88228	74.2932248	-0.122217633
5	5.6302	104.0105147	-0.178146185
4	4.50416	130.0131434	-0.227135573
3	3.37812	173.3508579	-0.3074847
2	2.25208	260.0262868	-0.463734016

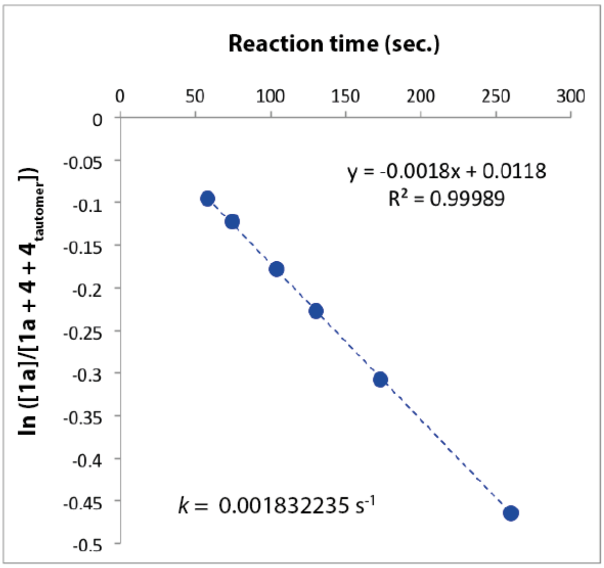

2.0 Equiv. EtOH			
Set flow (mL min^{-1})	Effective flow (mL min^{-1})	Reaction time (sec.)	ln([**1a**]/[**1a** + **4** + **4**$_{tautomer}$])
9	10.13436	57.78361929	-0.09531018
7	7.88228	74.2932248	-0.122217633
5	5.6302	104.0105147	-0.186479567
4	4.50416	130.0131434	-0.235072122
3	3.37812	173.3508579	-0.311154429
2	2.25208	260.0262868	-0.473123757

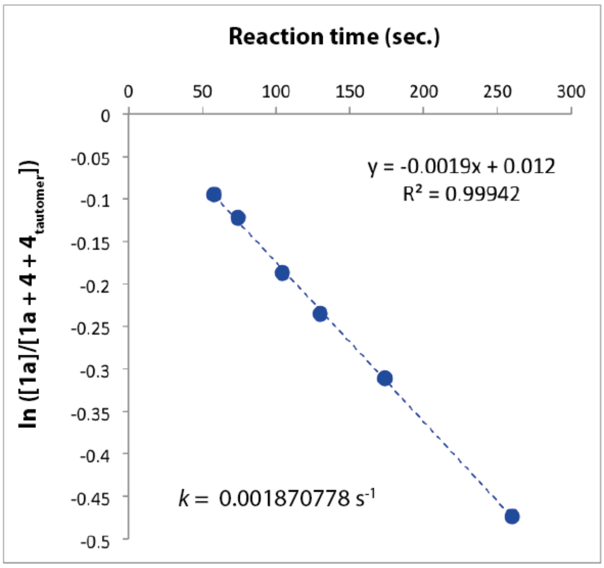

4.0 Equiv. EtOH			
Set flow (mL min^{-1})	Effective flow (mL min^{-1})	Reaction time (sec.)	ln([**1a**]/[**1a** + **4** + **4**$_{tautomer}$])
7	7.88228	74.2932248	-0.131028262
5	5.6302	104.0105147	-0.19062036
4	4.50416	130.0131434	-0.235072122
3	3.37812	173.3508579	-0.31481074

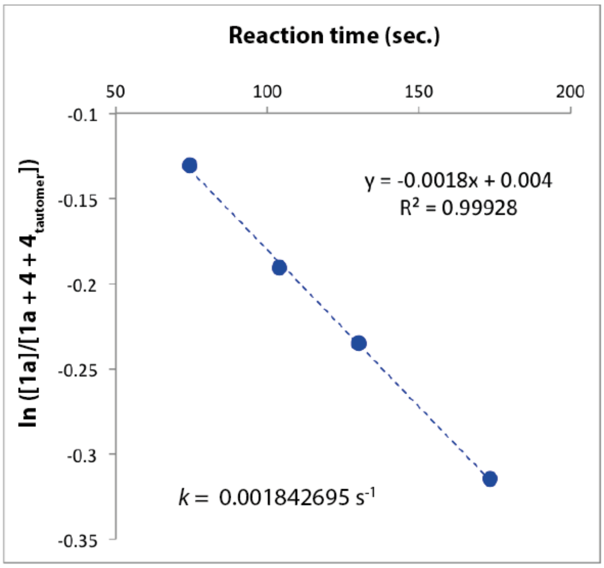

6. Synthesis and Characterisation of 1,3-Dioxin-4-ones

Compound **1a** was purchased from Sigma Aldrich®. The preparation and characterisation of **1b**,[2] **1e**,[3] **1f**,[3] **1g**,[3b] **1h**[3a] and **1i**[4] was carried out according to reported literature procedures. Compounds **1c** and **1d** were prepared by the same method and details of their synthesis and characterisation are given below in sections 6.1 and 6.2.

6.1 Characterisation Methods

NMR spectra were obtained on a Bruker AV300 or DPX400 MHz spectrometer as stated. ^{1}H chemical shifts are reported as values in ppm referenced to residual solvent. The following abbreviations are used to assign multiplicity: s = singlet, d = doublet. Coupling constants, *J*, are measured in Hertz (Hz). ^{13}C spectra are proton decoupled and referenced to solvent. ^{13}C resonances are reported as C, CH, CH_2 or CH_3 depending on the number of directly attached protons (0, 1, 2, 3 respectively) as determined by DEPT experiments. UV measurements were recorded in MeCN on an Ocean Optics DH-2000-BAL spectrometer integrated into the flow line with a type 583-F Starna® fluorimeter flow cell (1 mm path length, 0.011 mL volume). Electrospray mass spectra (ES) were recorded in CH_3CN using a VG platform quadrupole spectrometer.

Accurate mass spectra were recorded on a Bruker Apex III mass spectrometer using electrospray ionisation. Values of *m/z* are reported in atomic mass units. Infrared spectra for compound characterisation were run as neat films on a Thermo Nicolet 380 FT-IR spectrometer with a Smart Orbit Goldengate attachment. Absorptions are given in wavenumbers (cm^{-1}). Peaks are recorded as s (strong), m (medium), w (weak), sh (shoulder) and br (broad).

6.2 Synthesis and Characterisation of 1c and 1d

2-(4-methoxyphenyl)-2,6-dimethyl-4*H*-1,3-dioxin-4-one (**1c**)

To a solution of *tert*-butyl acetoacetate (5 mL, 30.15 mmol) and 4-methoxyacetophenone (9.06 g, 60.3 mmol) in acetic anhydride (10 mL, 106.44 mmol) at -10 °C, was added concentrated sulfuric acid (1.61 mL, 30.15 mmol) dropwise. During the addition, the temperature increased to 0 °C and the mixture was then allowed to warm to 15 °C before stirring for 16 h at this temperature. The mixture was then carefully transferred to an ice-cooled saturated (aqueous) solution of potassium carbonate (70 mL) and stirred for 30 min at room temperature. The aqueous layer was separated and extracted with CH_2Cl_2 (100 mL followed by 2 × 50 mL), the organic layers were then combined, washed with brine (3 × 50 mL) and dried over $MgSO_4$ before removal of solvents *in vacuo*. Purification by column chromatography (SiO_2 eluted with 10% *v/v* EtOAc in hexane) followed by crystallisation from hexane gave the title compound as a yellow powder (1.41 g, 20%).

^{1}H NMR (400 MHz, $CDCl_3$) δ = 1.87 (3H, s), 2.00 (3H, s), 3.81 (3H, s), 5.17 (1H, s, fine splitting), 6.89 (2H, d, *J* = 8.6 Hz), 7.38 (2H, d, *J* = 8.6 Hz) ppm. ^{13}C NMR (75 MHz, $CDCl_3$) δ = 20.07 (CH_3), 29.55 (CH_3), 55.31, (CH_3), 96.44 (CH), 106.68 (C), 113.88 (CH), 126.27 (CH), 132.50 (C), 160.05 (C), 161.46 (C), 168.95 (C) ppm. UV λ 230.50 nm e 10966 M^{-1} cm^{-1}; λ 245.88 nm e 7725 M^{-1} cm^{-1}. IR ν_{max} cm^{-1} 1710 (m), 1351 (m), 1244 (m), 1163 (m), 840 (m). LCMS (ESI+ *m/z*) 235, 100% $(M+H)^+$; 257, 10% $(M+Na)^+$. HRMS (ESI+ *m/z*): Found 257.0783 ($M+Na^+$), calculated for $C_{13}H_{14}NaO_4^+$ 257.0784.

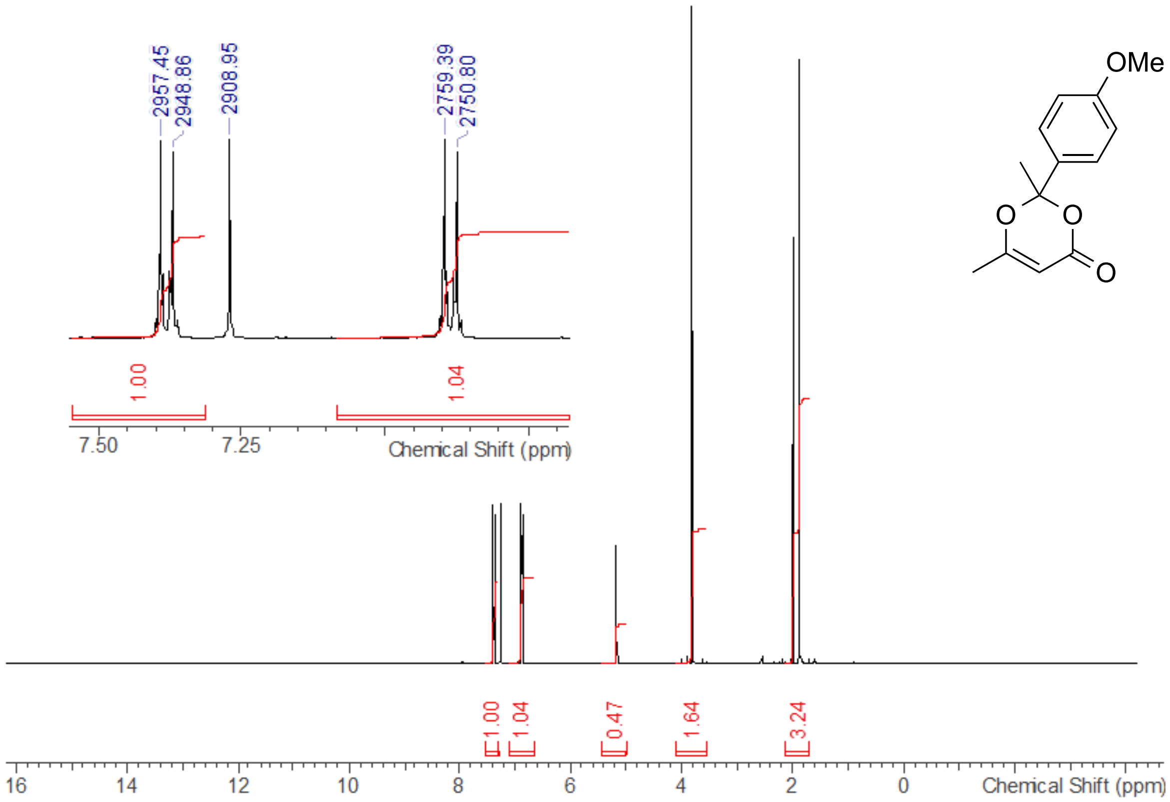
2957.45
2948.86
2908.95
2759.39
2750.80
1.00
1.04
7.50
7.25
Chemical Shift (ppm)
OMe
O
O
O
1.00
1.04
0.47
1.64
3.24
16
14
12
10
8
6
4
2
0
Chemical Shift (ppm)

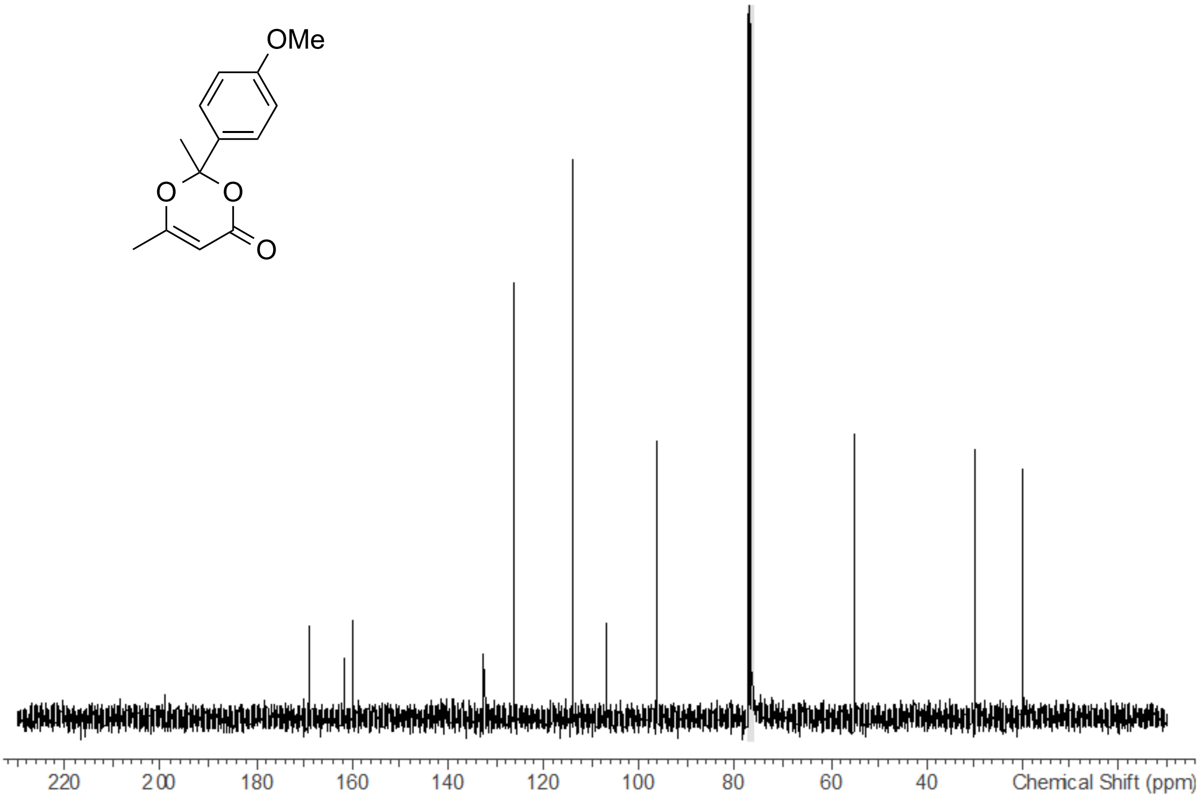
OMe
O
O
O
220
200
180
160
140
120
100
80
60
40
Chemical Shift (ppm)

2-(4-bromophenyl)-2,6-dimethyl-4*H*-1,3-dioxin-4-one (**1d**)

To a solution of *tert*-butyl acetoacetate (2.0 mL, 12.06 mmol) and 4-bromoacetophenone (4.88 g, 24.52 mmol) in acetic anhydride (4.03 mL, 42.58 mmol) at -10 °C, was added concentrated sulfuric acid (0.65 mL, 12.06 mmol) dropwise. During the addition, the temperature increased to 0 °C and the mixture was stirred for 43 h at this temperature. The mixture was then carefully transferred to an ice-cooled saturated (aqueous) solution of potassium carbonate (50 mL) and stirred for 30 min at room temperature. The aqueous layer was separated and extracted with CH_2Cl_2 (3 × 100 mL), the organic layers were combined, washed with brine (3 × 100 mL) and dried over $MgSO_4$ before removal of solvents *in vacuo*. Purification by column chromatography (SiO_2 eluted with 15% *v/v* Et_2O in hexane) gave the title compound as a white powder (0.60 g, 18%).

^{1}H NMR (400 MHz, $CDCl_3$) δ 1.87 (3H, s), 2.01 (3H, s), 5.18 (1H, s, fine splitting), 7.34 (2H, d, *J*= 8.8 Hz), 7.51 (2H, d, *J*= 8.8 Hz) ppm. ^{13}C NMR (100.5 MHz, $CDCl_3$) δ 20.05 (CH_3), 29.33 (CH_3), 96.63 (CH), 106.16 (C), 123.35 (C), 126.70 (CH), 131.86 (CH), 139.66 (C), 160.90 (C), 169.00 (C) ppm. UV λ 229.75 nm e = 12161 $M^{-1}cm^{-1}$; λ 246.63 nm e = 7898 $M^{-1}cm^{-1}$. IR ν_{max} cm^{-1} 1716 (m), 1387 (m), 1171 (m), 969 (m), 824 (s). LCMS (ESI+ *m/z*) 283, 100% $[M(^{79}Br)+H]^+$; 285, 100% $[M(^{81}Br)+H]^+$; 305, 20% $[M(^{79}Br)+Na]^+$; 307, 20% $[M(^{81}Br)+Na]^+$. HRMS (ESI+ *m/z*): Found 304.9786, calculated for $C_{12}H_{11}BrNaO_3^+$ 304.9784.

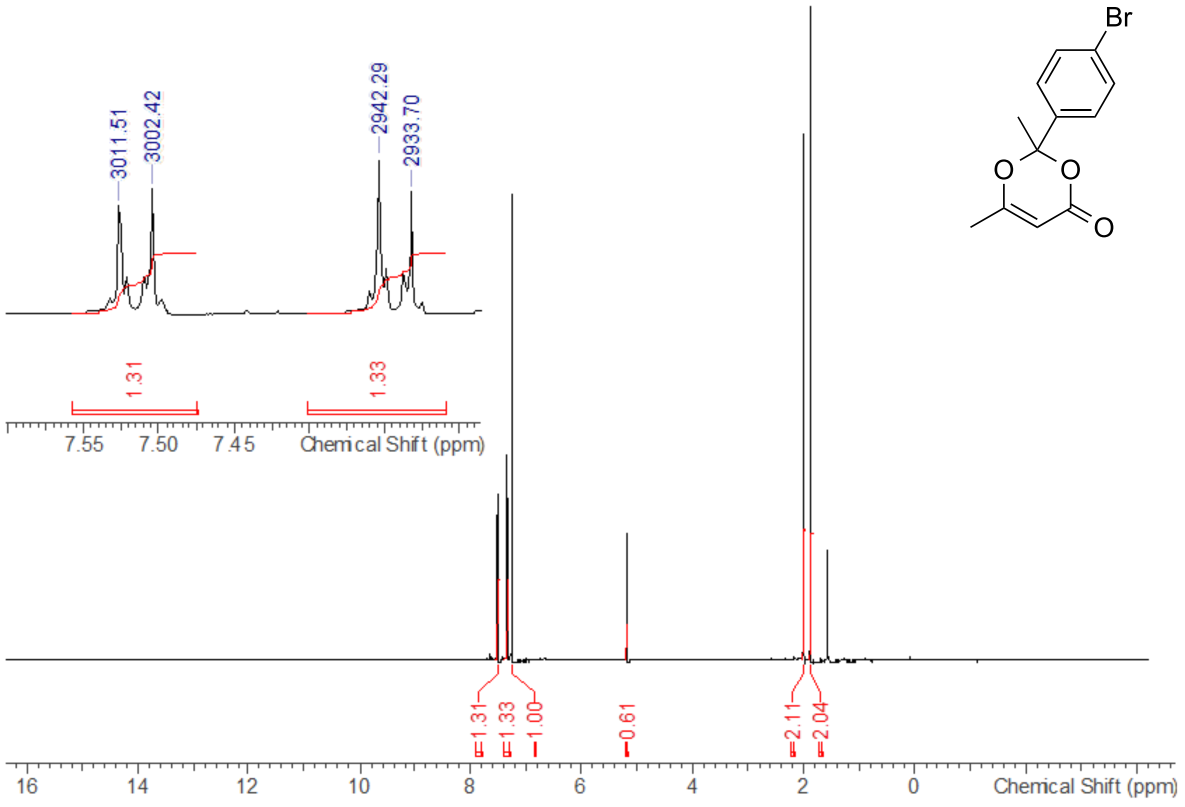

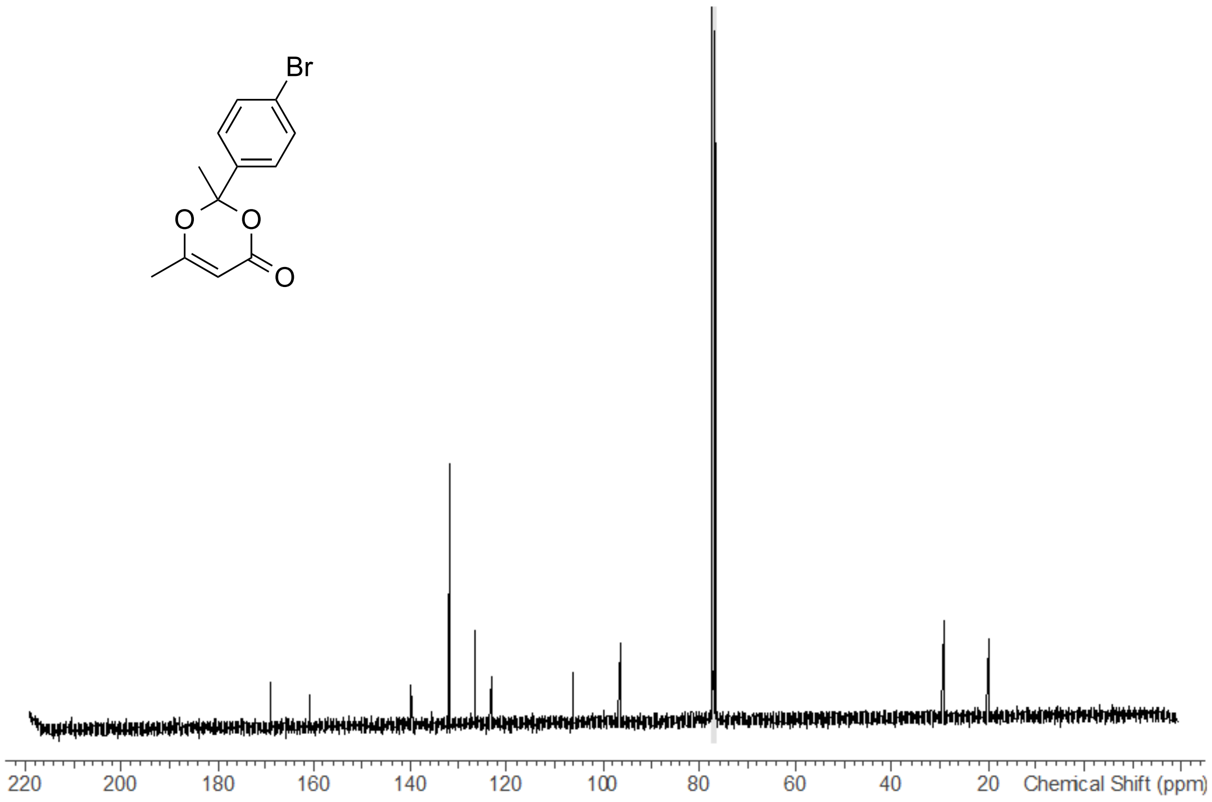

7. Dispersion Experiments

7.1 Experimental Dispersion Profiling

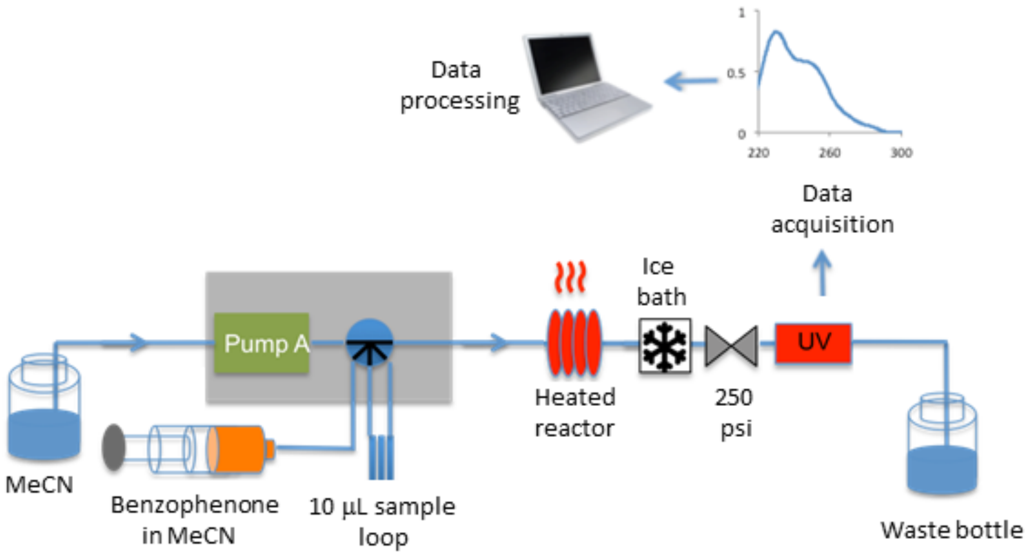

Figure S7.1 Schematic of flow set-up utilising a single channel (Pump A) of the Vapourtec R series platform and bottle-feed with a 10 µL injection loop configuration, 10 mL stainless steel reactor submerged in a precision oil bath, ice bath cooling of the reactor efflux, 250 psi back-pressure regulation and in-line UV data acquisition.

Dispersion profiles were obtained at 30 °C and 120 °C and at flow rates between 0.1 and 10 mL min^{-1} using the experimental set-up described in Figure S7.1. For each experiment, 10 µL of a solution of benzophenone in MeCN ($[C_0] = 1.015 \times 10^{-2}$ M) was injected via the sample loop and pushed with the carrier solvent MeCN. In-line UV detection was used and calibration-less calculation of [benzophenone]/$[\text{benzophenone}]_0$ was made by integration of the 250 nm peak in the UV spectrum with respect to 0% conversion using Bristol Online Reaction Investigation Software (BORIS). UV absorbance was converted into molar units using a calibration curve (Figure S7.2).

In order to compare the dispersion at each individual flow rate: volume eluted (mL) = time (min) × flow rate (mL min^{-1}). Correction for thermal expansion of solvent is calculated according to: $\text{Flow}_{\text{actual}} = \text{Flow}_{\text{pump display}} (1 + \alpha\Delta T)$ where α = the expansion coefficient of solvent.

Dispersion curves obtained at 30 °C and 120 °C are given in Figures S7.3 and S7.4, respectively.

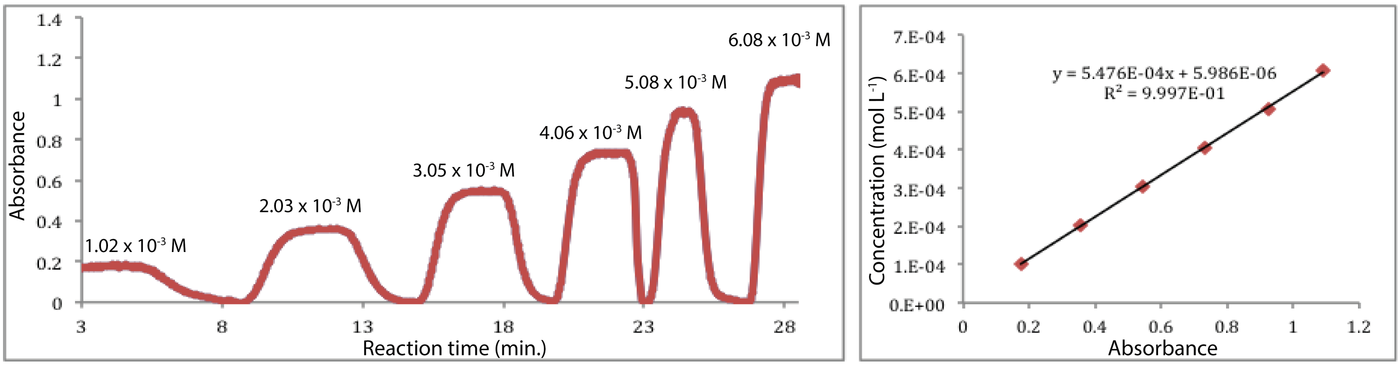

Figure S7.2 Calibration curve to convert UV absorbance of benzophenone solutions into molar concentration (mol/L)

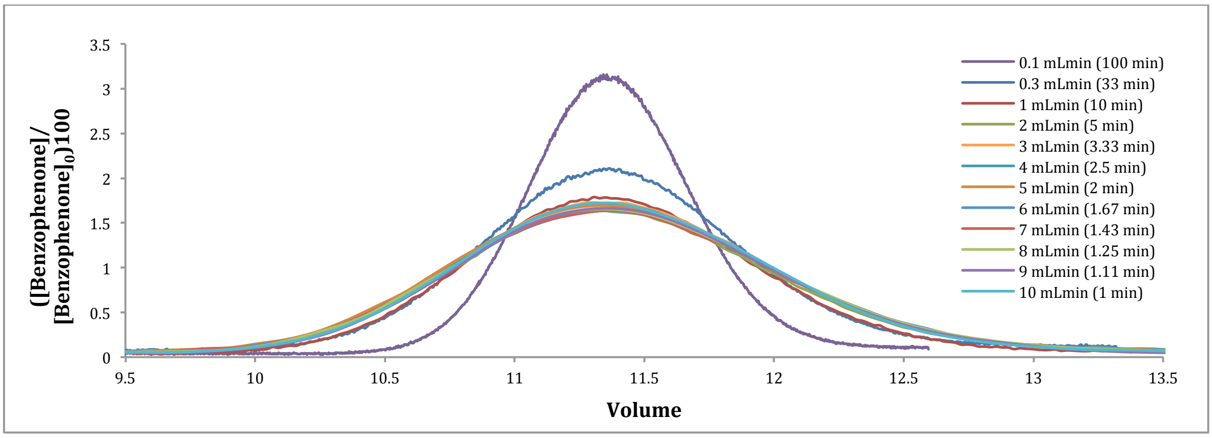

Figure S7.3 Dispersion of a 10 μL sample plug of benzophenone in MeCN ($[C]_0 = 1.015 \times 10^{-2}$ M) through coiled stainless steel tubing of 1 mm internal diameter and 10 mL capacity at 30 °C and the flow rates indicated.

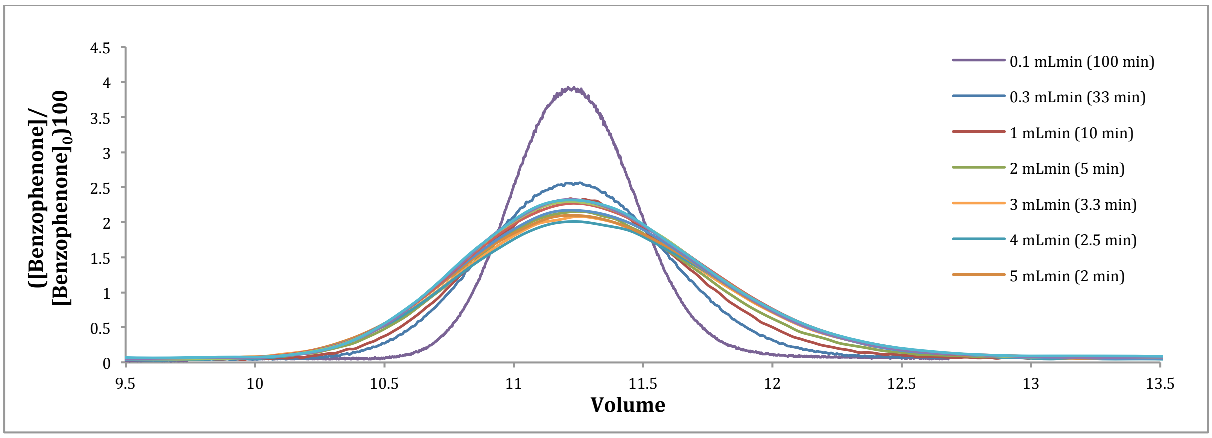

Figure S7.4 Dispersion of a 10 μL sample plug of benzophenone in MeCN ($[C]_0 = 1.015 \times 10^{-2}$ M) through coiled stainless steel tubing of 1 mm internal diameter and 10 mL capacity at 120 °C and the flow rates indicated.

7.2 Simulated dispersion effects upon 1st and 2nd order kinetics

Reagent concentration profiles were calculated for a theoretical 1st order reaction (A → P) and 2nd order reaction (2A → P) under push-out conditions of stepped flow-rate from 1 ml min^{-1} to 10 mL min^{-1} with flow rate switching at experimental time t = 0 (reaction time = 10 min.). Figures S7.5(a) and S7.6(a) show the calculated profiles.

The dispersion profile obtained at 10 mL min^{-1} and 30 °C for benzophenone (Figure S7.3) was then used to simulate the effect of dispersion upon each data point of the calculated reagent concentration profiles. Figures S7.5(b) and S7.6(b) show the resulting simulated profiles.

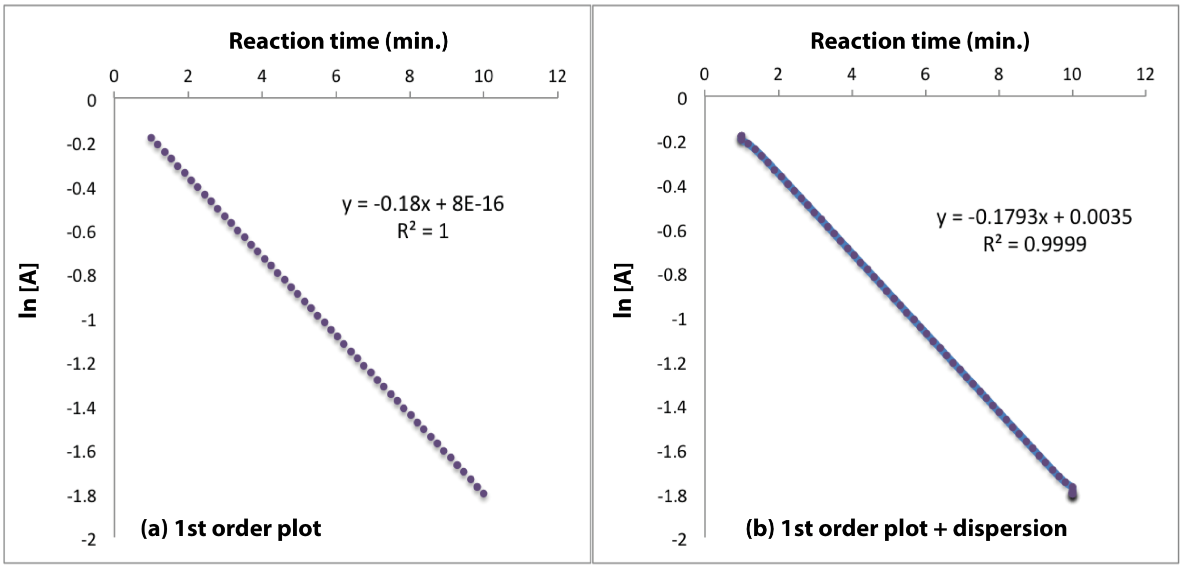

Figure S7.5

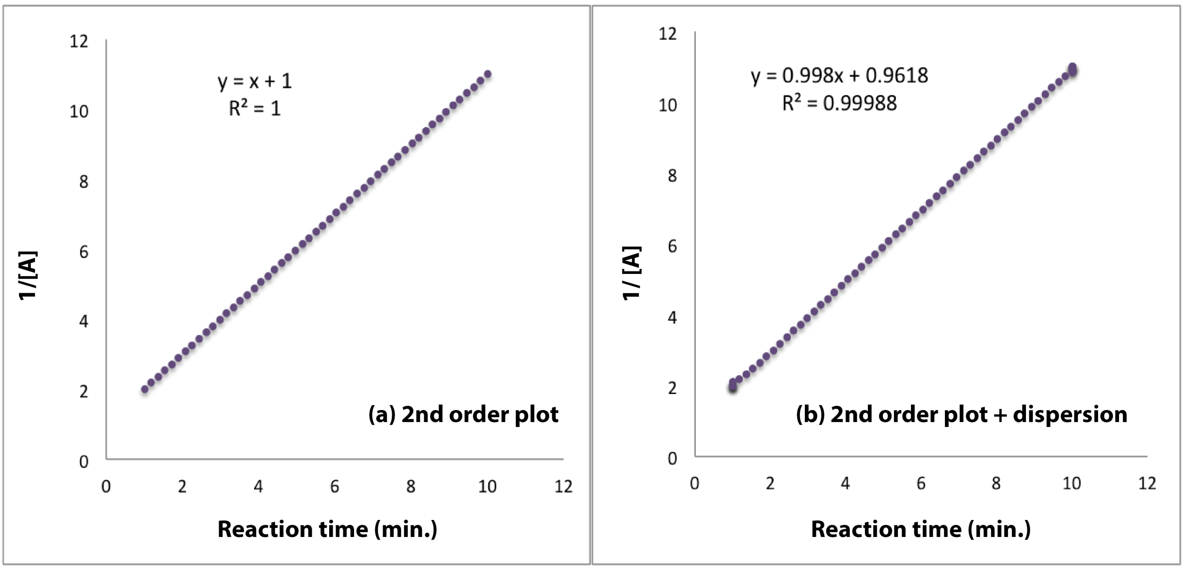

Figure S7.6

8. References

[1] H. A. Zarei, M. Z. Lavasani, H. Iloukhani, *J. Chem. Eng. Data* **2008**, *53*, 578-585.

[2] N. Haddad, I. Rukhman, Z. Abramovich, *J. Org. Chem.* **1997**, *62*, 7629-7636.

[3] a) P. A. Peixoto, A. Boulangé, S. Leleu, X. Franck, *Eu.r J. Org. Chem.* **2013**, 3316-3327; b) M. Sato, H. Ogasawara, K. Oi, T. Kato, *Chem. Pharm. Bull.* **1983**, *31*, 1896-1901.

[4] A. Boulangé, P. A. Peixoto, X. Franck, *Chem. Eur. J.* **2011**, *17*, 10241-10245.